NTNU
Det skapende universitet

Olje-vann separasjon i rør

Henrik Eiane Heggebø

Produktutvikling og produksjon
Innlevert: Juni 2012
Hovedveileder: Ole Jørgen Nydal, EPT

Norges teknisk-naturvitenskapelige universitet
Institutt for energi- og prosessteknikk

NTNU

Norges teknisk-
naturvitenskapelige universitet
NTNU

Institutt for energi- og prosessteknikk

EPT-M-2011-4034

MASTEROPPGAVE

for

Studentene Henrik Eiane Heggebø og Asbjørn Øye Gjerde

Våren 2012

Oil-water separation in inclined pipes
Olje-vann separasjon i rør

Bakgrunn

Når en strømmende olje-vann blanding i et rør stanser opp, vil oljen og vannet separeres. Etter en separasjonstid med motstrøms olje-vann strøm vil vannet samles nederst i røret, og oljen øverst. Separasjonstiden avhenger av strømningsmønsteret, blandet strøm har lenger separasjonstid enn separert strøm.
Det er behov for enkle beregningmodeller for en-dimensjonal, motstrøms olje-vann strøm. Slike modeller anvendes i dynamiske strømningssimulatorer for olje-vann-gass i rør. Ved EPT arbeides det også med frontfølgemodeller, der realistiske sliprelasjoner for motstrøms olje-vann strøm mangler.
Det er en utfordring å utføre detaljmålinger i motstrøms olje-vann strøm. Ofte kan enkle forsøk kunne gi verdifull informasjon og være til hjelp i formulering av modeller. Et enkelt oppsett vil være et rør med olje vann. Når helningen endres hurtig, vil separasjonsforløpet deretter kunne observeres visuelt (video) og separasjonstiden måles.

Mål

Det skal utføres dynamiske forsøk med separasjon av olje og vann i rør. Et rør får en vinkelendring fra et utgangpunkt (horisontalt eller vertikalt) og det påfølgende separasjonsforløpet skal registreres for mange vinkelendringer og for flere typer oljer. Observasjonene skal danne grunnlaget for formulering av enkle separasjonsmodeller som kan anvendes i en strømningssimulator.

Oppgaven bearbeides ut fra følgende punkter

1. Litteraturoversikt over problemstillingen
2. Etablering av et forsøksoppsett
3. Utførelse av forsøk
4. Evaluering av data med hensyn på enkle modeller
5. Rapportering om mulig i form av vitenskapelig publikasjon

Senest 14 dager etter utlevering av oppgaven skal kandidaten levere/sende instituttet en detaljert fremdrift- og eventuelt forsøksplan for oppgaven til evaluering og eventuelt diskusjon med faglig ansvarlig/veiledere. Detaljer ved eventuell utførelse av dataprogrammer skal avtales nærmere i samråd med faglig ansvarlig.

Besvarelsen redigeres mest mulig som en forskningsrapport med et sammendrag både på norsk og engelsk, konklusjon, litteraturliste, innholdsfortegnelse etc. Ved utarbeidelsen av teksten skal kandidaten legge vekt på å gjøre teksten oversiktlig og velskrevet. Med henblikk på lesning av besvarelsen er det viktig at de nødvendige henvisninger for korresponderende steder i tekst, tabeller og figurer anføres på begge steder. Ved bedømmelsen legges det stor vekt på at resultatene er grundig bearbeidet, at de oppstilles tabellarisk og/eller grafisk på en oversiktlig måte, og at de er diskutert utførlig.

Alle benyttede kilder, også muntlige opplysninger, skal oppgis på fullstendig måte. For tidsskrifter og bøker oppgis forfatter, tittel, årgang, sidetall og eventuelt figurnummer.

Det forutsettes at kandidaten tar initiativ til og holder nødvendig kontakt med faglærer og veileder(e). Kandidaten skal rette seg etter de reglementer og retningslinjer som gjelder ved alle (andre) fagmiljøer som kandidaten har kontakt med gjennom sin utførelse av oppgaven, samt etter eventuelle pålegg fra Institutt for energi- og prosessteknikk.

Risikovurdering av kandidatens arbeid skal gjennomføres i henhold til instituttets prosedyrer. Risikovurderingen skal dokumenteres og inngå som del av besvarelsen. Hendelser relatert til kandidatens arbeid med uheldig innvirkning på helse, miljø eller sikkerhet, skal dokumenteres og inngå som en del av besvarelsen.

I henhold til "Utfyllende regler til studieforskriften for teknologistudiet/sivilingeniørstudiet" ved NTNU § 20, forbeholder instituttet seg retten til å benytte alle resultater og data til undervisnings- og forskningsformål, samt til fremtidige publikasjoner.

Besvarelsen leveres digitalt i DAIM. Et faglig sammendrag med oppgavens tittel, kandidatens navn, veileders navn, årstall, instituttnavn, og NTNUs logo og navn, leveres til instituttet som en separat pdf-fil. Etter avtale leveres besvarelse og evt. annet materiale til veileder i digitalt format.

NTNU, Institutt for energi- og prosessteknikk, 16. januar 2012

Olav Bolland
Instituttleder

Ole Jørgen Nydal
Faglig ansvarlig/veileder

Medveileder(e) Tor Kjeldby (PhD)

Abstract/*Sammendrag*

Transient counter-current gravity driven oil-water flow experiments were conducted in a 2 meter long enclosed plexiglas cylinder. A simple experimental setup based on visual inspection was constructed for the purpose of this research. Experiments were performed with a wide range of inclinations between 0 and 90 degrees from the horizontal. The effects of different experimental parameters were investigated using two types of oil, Exxsol D80 and Marcol 52; two cylinder inner diameters, 50mm and 90mm; as well as three water cuts, 0.25, 0.5 and 0.75. To simulate a broad spectrum of flow situations, three different starting conditions with varying degrees of mixing were used. A total of 755 experiments were conducted during this research.

The results have been used to develop slip relations that will be implemented in a slug tracking simulator being developed at the Norwegian University of Science and Technology. Four different flow patterns have been identified in this research. Only small deviations in flow patterns were observed when cylinder diameter or oil phase were altered. Inclinations between 15 and 30 degrees were found to yield the highest slip velocities.

Transiente motstrøms tyngdekrafts-drevne olje-vann strømningsforsøk ble gjort i en to meter lang lukket plexiglass sylinder. Et enkelt eksperimentelt oppsett baser på visuelle observasjoner ble laget med formål for disse forsøkene. Eksperimenter ble gjort for et stort utvalg av inklinasjoner mellom 0 og 90 grader fra horisontalen. Effektene av ulike eksperimentelle parametere ble undersøkt ved å bruke to typer olje, Exxsol D80 og Marcol 52, to sylindere med ulik indre diameter, 50mm og 90mm, i tillegg til tre ulike vannkutt; 0,25, 0,5 og 0,75. For å simulere et bredt utvalg av strømnings situasjoner ble det brukt tre ulike start kondisjoner med varierende grad av miksing av innholdet. Totalt ble det gjort 755 eksperimenter i løpet av denne oppgaven.

Resultatene fra observasjonene har blitt brukt til å danne slip relasjoner som skal bli implementert i en slug-tracking simulator som blir utviklet ved NTNU. Fire ulike strømningsmønster har blitt identifisert for denne type strømning. Kun små forskjeller i strømningsmønster ble observert for ulike olje faser og sylinder diametere. Helninger mellom 15 og 30 grader ble funnet til å gi høyest slip hastighet mellom olje og vann fasene.

Preface

This master thesis was carried out for the department of Energy and Process Engineering at the Norwegian University of Science and Technology, NTNU, during the spring semester of 2012. The experiments for this thesis were conducted at the multiphase laboratory.

We would like to thank our supervisor Professor Ole Jørgen Nydal for introducing us to this subject, for the support we have received during this thesis. We would also like to that our co supervisor PhD student Tor Kjeldby for offering valuable knowledge on this subject and also for his great effort in helping us erect the experimental setup.

Table of Contents

List of Figures

List of tables

Nomenclature

Symbol		Unit
α_o	In situ oil phase fraction	(-)
α_w	In situ water phase fraction	(-)
A	Pipe cross section area	(m^2)
A_o	Area occupied by oil phase	(m^2)
A_w	Area occupied by water phase	(m^2)
Cw	Water cut	(-)
D	Diameter	(mm)
ID	Inner Diameter	(mm)
ν	Kinematic viscosity	(mm^2/s)
ρ_o	Density oil	(kg/m^3)
ρ_w	Density water	(kg/m^3)
σ	Interfacial tension	(mN/m)
σ_s	Standard deviation	(-)
θ	Degree of inclination	(º)
t	Time	(s)
t_{end}	End time	(s)
t_{start}	Starting time	(s)
$t_{o,e}$	Time for oil to reach the end	(s)
$t_{w,e}$	Time for water to reach the end	(s)
t_{sep}	Separation time	(s)
u_b	Control volume border velocity	(m/s)
$u_{bo\ avg}$	Average oil front velocity	(m/s)
$u_{bw\ avg}$	Average water front velocity	(m/s)
u_o	Oil phase velocity	(m/s)
u_w	Water phase velocity	(m/s)
u_s	Slip Velocity	(m/s)
V_{tot}	Total Volume	(m^3)
V_w	Volume of Water	(m^3)

1 Introduction

As more and more oil reservoirs are reaching a mature stage, high water production is becoming a common occurrence. Therefore there has been put increased effort into optimizing the current pipeline and production systems to be able to handle flow with high water content to ensure efficient operation. This requires accurate and reliable models that incorporate multiphase flow for pipeline and riser system simulation tools.

In general there are three approaches for developing such simulation tools. Empirical correlations, which are based on purely experimental data are limited to the conditions used in the experiments and can often be difficult to relate to various real cases. Mechanistic models, which are based on physical relations, are often believed to be the most accurate. However, they are very complicated, requiring long computational time and may cause discontinuities at transitions between flow patterns. Homogeneous models, which are based on representing all the phases in the system by a single mixed phase, which are relatively simple compared to mechanistic models, but could be less accurate. These models can incorporate slip relations between the phases based on experimental data and are often referred to as drift flux models (Durlofsky & Aziz, 2004). Using this method removes the requirement for closure relations between the phases in terms of interface friction factors.

A slug tracking simulator based on using a mixture liquid momentum formulation is being developed at the Norwegian University of Science and Technology. This simulator requires empirical data on slip relations for situations where counter-current flow is encountered. This encompasses situations where the overall flow velocity is very small or even stagnant, for example when the production is stopped during a system shutdown. Since water and oil generally are immiscible liquids, they will separate and in inclined situations the heavy phase will sink downwards while the light phase rises upwards. Even though a lot of research has been conducted on multiphase flow, little effort has been put into this specific area (Fairuzov, 2003). Therefor new experimental data is needed in the case of counter-current oil-water flow. It has also been implied that precise characterization of flow patterns involving counter-current flow is necessary for improving the interpretation of production logs (Flores, Chen, Sarica, & P, 1999).

For the purpose of developing slip relations for counter-current flow, a simple experimental setup based on visual inspection of oil and water flow has been constructed. The experiments are based on an enclosed cylinder filled with water and mineral oil which is rotated and set at a desired angle. This creates a transient counter-current flow pattern that can be studied visually. A range of experimental parameters can easily be altered; the setup allows for experiments at any angle of inclination, different mineral oils, any water cut and different cylinder diameters. In addition to this, three different starting conditions are tested which simulate different degrees of mixed flow as well as separated flow.

2 Background

2.1 Definitions

The slip velocity between oil and water in an immiscible liquid-liquid system can be defined as the difference between the oil and water velocity as expressed in Equation 2.1.

$$u_s = u_o - u_w \qquad \text{Equation 2.1}$$

Where u_s, u_o and u_w represent the slip, oil and water velocities respectively. Figure 1 below illustrates a simplified oil-water flow in a small segment in an inclined pipe structure. A control volume is taken around the boundary between the two phase oil-water section and the single phase water section. This boundary is referred to as the oil-waterfront. It is assumed that the control volume border velocities as well as the oil-water front velocities are equal and are denoted u_b. The pipe segment inclination from the horizontal is represented by θ, while the x is the abscissa along the pipe length axis.

The water cut, C_w, is defined by dividing the volume of water, V_w, by the total volume, V_{tot}, in Equation 2.2.

$$C_W = \frac{V_w}{V_{tot}} \qquad \text{Equation 2.2}$$

The in situ fractions of each phase are denoted as α_o and α_w and are defined in Equation 2.3.

$$\alpha_o = \frac{A_o}{A} \qquad \alpha_w = \frac{A_w}{A} \qquad \text{Equation 2.3}$$

Where A is the total cross section area of the pipe and A_o and A_w represent the area occupied by the oil and water phase.

The conservation of mass for oil is given in Equation 2.4 and similarly for water in Equation 2.5.

$$\frac{\partial \alpha_o \rho_o}{\partial t} + \frac{\partial \alpha_o \rho_o (u_o - u_b)}{\partial x} = 0 \qquad \text{Equation 2.4}$$

$$\frac{\partial \alpha_w \rho_w}{\partial t} + \frac{\partial \alpha_w \rho_w (u_w - u_b)}{\partial x} = 0 \qquad \text{Equation 2.5}$$

Assuming that the densities of oil and water, ρ_o and ρ_w, are constant, integration over the control volume yields the following relation in Equation 2.6.

$$[\alpha_o(u_o - u_b) + \alpha_w(u_w - u_b)]_2 - [\alpha_o(u_o - u_b) + \alpha_w(u_w - u_b)]_1 = 0 \qquad \text{Equation 2.6}$$

In an ideal situation it can be assumed that the oil velocity at node 2, u_{o2}, is equal to the control volume border velocity, u_b. In node 1, where there is a single phase water section, the water velocity, u_{w1} is zero and the oil fraction α_{o1} is zero. Substituting these assumptions in

Equation 2.6 and introducing the slip velocity in Equation 2.1 leads to the simple slip velocity Equation 2.7.

$$u_s = \frac{u_b}{\alpha_{w2}} \qquad \text{Equation 2.7}$$

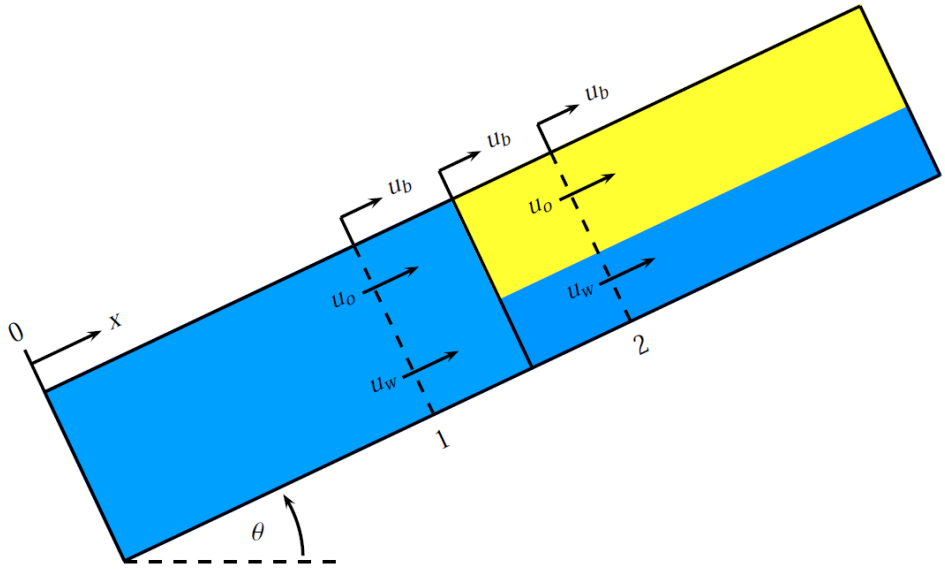

Figure 1 Control volume for calculation of experimental slip velocity.

2.2 Flow patterns

Little research is available on the matter of transient counter-current liquid-liquid flow in pipe-structures, making it difficult to predict what kind of flow patterns can be expected in the experiments of this research. However, there has been some research on laminar counter-current liquid-liquid flow and also the field of gas-liquid counter-current flows. It is not known if any results from these fields can be extrapolated to transient counter-current liquid-liquid flow.

2.2.1 Laminar counter-current liquid-liquid flow

The effects of inclination on the characteristics of laminar counter-current liquid-liquid flow have been investigated both experimentally and theoretically by (Ullmann, Zamir, Ludmer, & Brauner, 2003). In the experiments, a mixture of ethyl acetate, water and ethanol was used, forming two phases with a small density ratio. The Eötvös number was much higher than unity, giving a gravity dominated system. In a vertical position, the dominating flow pattern is dispersed flow as shown in Figure 2 a). At inclinations slightly off the vertical, the liquids were found to start separating, Figure 2 b). Inclinations higher off the vertical (about 30-40°) were found to result in a stratified counter-current flow with a stable interface, Figure 2 c).

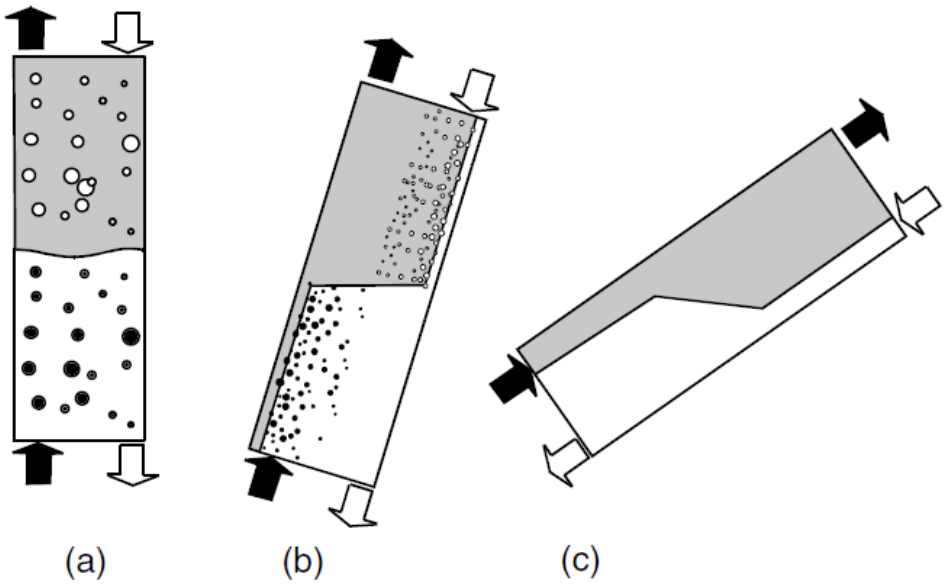

Figure 2 Laminar counter-current liquid-liquid flow patterns for various inclinations; a) vertical inclination, b) slightly off vertical inclination, c) higher inclination off vertical (Ullmann, Zamir, Ludmer, & Brauner, 2003)

2.2.2 Counter-current gas-liquid flow

Counter-current gas-liquid flow is often encountered in the petroleum industry and has been well studied. At vertical inclination, there are mainly three different flow patterns that appear. These are commonly referred to as annular flow, bubble flow and slug flow (Taitel & Barnea, 1983). Annular flow is characterized by the liquid flowing downwards along the surface of the wall, while the gas flows upwards as a continuous phase in the middle. Bubble flow is characterized by a continuous liquid phase with dispersed gas bubbles rising upwards through the liquid. Finally, slug flow consists of long Taylor bubbles that are separated by slugs of liquid which may contain gas bubbles. Another flow pattern that has been observed in large diameter pipes is called Turbulent Churn and can be put in a sub-category within Slug Flow (Taitel & Barnea, 1983). The subject is studied experimentally in the research by (Hasan, Kabir, & Srinivasan, 1994).

A study on counter-current gas-liquid flow in nearly horizontal pipes indicates that the dominating flow pattern at 10° inclination is stratified flow for several different types of liquid (Prayitno, Santoso, Deendarlianto, Höhne, & Lucas, 2012). Another experimental work using a small cylinder with an inner diameter of 19mm, studied counter-current two-phase gas-liquid flow at 0, 30 and 68° inclination from the vertical. A range of different liquids were used as the liquid phase. With water as the liquid phase at a vertical inclination, the major flow patterns observed were; bubbly, slug, churn and churn-annular, depending on the superficial phase velocities. At off-vertical inclinations however, the dominating flow patterns were slug, churn-stratified and semi-stratified. Using mineral and paraffinic oils as the liquid phase, slug, slug-froth and froth were the dominating flow patterns for all tested inclinations. The froth flow pattern was characterized by a chaotic regime with no discernible gas-liquid interface configuration. The slug-froth flow pattern was composed of Taylor bubbles separated by long regions of froth flow (Ghiaasiaan, Wu, Sadowski, & Abdel-khalik, 1997).

However, it has been suggested that the concepts and results from gas-liquid flows cannot be readily transferred to the liquid-liquid flows (Brauner & Maron, 1992).

2.2.3 Steady-state counter-current multiphase flow

Oil-water flow in inclined pipes is another subject that may yield some results that are applicable for this study. This type of flow is often encountered in wells and reservoir where the inclination of the pipes can vary from horizontal to vertical and everything in between. If the liquids are flowing at low superficial velocities, there may be local occurrences of counter-current flow where the water phase is moving downwards along the pipe wall. This behavior is only observed when water is the continuous phase and its range of occurrence is significantly affected by the angle of inclination (Flores, Chen, Sarica, & P, 1999).

2.2.4 Predicted Flow Patterns

Consider an enclosed cylinder containing two immiscible liquids, in this case water and oil which are initially completely separated. If the cylinder is initially in a horizontal position, then tilted to a certain angle, the oil will start flowing towards the elevated end of the cylinder and vice versa for the water phase. If the tilted angle is small, the liquids will flow will easily flow in a stratified manner since they are initially separated. The larger the tilt, the more disturbed and chaotic the flow will become with increasing wave formation.

If the cylinder is initially in a vertical position with the two phases completely separated, and the cylinder is now tilted more than 90°, the phases will be blocking each other's paths. It is therefore reasonable to assume that the flow will be more chaotic compared to the previous example. At low inclinations, the oil phase will be tending to flow along the top side of the cylinder, while the water phase seeks to flow along the bottom. Thus it is expected to have tendencies towards stratified flow. As the angle increases towards a vertical position again (180° tilt), this channeling effect will diminish and the phases will be completely blocking each other. Therefore it is expected that the phases will hinder each other more and that the effect of friction will increase.

In a case where the phases are initially completely mixed, the phases will seek to separate from each other. If the cylinder is in a horizontal position, the separation is expected to be rather quick, since the distance required to travel for each phase is small. If the cylinder is in a vertical position, the water at the very top of the pipe will have a much longer distance to travel, assuming that the length of the cylinder is much greater than the diameter. At any angle in between it is expected that channeling will have a greater impact as the deviation from the horizontal increases.

2.3 Experimental parameters

Considering liquid-liquid counter-current flow in an enclosed volume, the dominating forces acting within the system are gravity and friction. Any flow occurring will be gravity driven and the velocity of the flow will be balanced by friction forces. At inclined flow, there will always be a gravity force component acting in the direction normal to the flow, forcing the heavy liquid phase towards the bottom and the light liquid towards the top. The other gravity force component will act in the direction parallel to the flow. As long as there is a density difference between the two liquids, the gravity force will act to separate the liquids. At low

inclinations, the liquids will separate quickly in the direction normal to the flow, but more slowly in the parallel direction. The outer points are the horizontal position where the phases will separate, but there will be no flow in the length direction of the pipe, and the vertical position where there will be no separation in the direction normal to the cylinder, or no channelization.

The friction force can be split in two major components; wall friction and interface friction between the two liquids. The wall friction will depend on the liquid and wall properties, liquid-wall contact area as well as the liquid velocity near the wall. The effects of wall friction increase with higher liquid velocities, higher wall roughness and smaller pipe diameter, due to increased circumference to cross-section ratio. No purely theoretical model for liquid-wall friction is currently available (Wongwises, 1998). The interface friction will depend on the liquid properties, slip velocity and on the flow regime. This makes the interface friction force very complex to deal with since the slip velocity is depending on the friction and since the flow pattern is depending on a number of factors, the inclination of the cylinder being a major one of these. As suggested earlier, the flow will become more dispersed at higher inclinations and certainly for vertical flow. Any change in flow pattern that increases the contact area between the two liquids will lead to increased interface friction. Establishing a mechanistic model for predicting the magnitude of the friction forces in counter-current liquid-liquid flow is thereby a highly complicated matter and no such models are available.

Nevertheless it can be assumed that the friction force, acting the opposite direction of the flow, will increase in magnitude with increasing inclination due to the reasons mentioned above. The gravitational force acting in the direction of the flow will also increase with the angle of inclination. The slip velocity will be a function of these two forces and the maximum velocity will be found at some inclination where sum of those forces is the highest.

2.3.1 Oil Phase Properties

The separation process is highly dependent on the density difference between the phases. Increasing difference in density between the phases will lead to faster separation and higher front velocities. This will in turn cause increased turbulence and mixing of the phases.

The oil phase viscosity can vary significantly between different oil fields and can impact both the mixing and the separation process. Recent research by (Yusuf, et al., 2011) found that oil has an increased tendency to disperse in water at low oil viscosities. The research was performed on horizontal co-current pipe flow. (Vedapuri, Bessette, & Jepson, 1997) found that high oil viscosity yielded a smaller degree of mixing and generally observed less amount of water penetrating the oil phase. When the flow pattern is dispersed and water is the continuous phase, the oil viscosity has little impact on the flow behavior (Arirachakaran, Oglesby, Malinowsky, Shoham, & Brill, 1989).

2.3.2 Wall properties

There is a significant difference in flow patterns and phase distribution depending on the pipe material used. A study by (Angeli, Pressure Drop and Flow Patterns in Horizontal Liquid-Liquid Flow in Pipes, 1994) suggested that transition between flow regimes is dependent on pipe wall roughness. An increased tendency towards dispersions in stainless steel tubes

compared to acrylic tubes was observed by (Angeli & Hewitt, Flow structure in horizontal oil-water flow, 2000). Therefore it is desirable to perform experiments with a steel cylinder to replicate a real situation, but this is not possible in experiments that are based on visual inspection.

2.3.3 Pipe Diameter

Most of the existing available empirical data on the subject of counter-current flow is based on experiments using small diameter pipes (2inches or less) (Durlofsky & Aziz, 2004). As most production and transport pipelines are larger than this, the empirical data obtained from such experiments may not be applicable in simulations of real production equipment. It has been found for gas-liquid flow in horizontal pipes that different pipe diameters with the same superficial velocities can yield different flow patterns (Jepson & Tayler, 1993) (Shi, et al., 2005). The effect of pipe diameter on flow pattern has also been observed in experimental research using 50 and 25 mm ID pipes with horizontal flow (Xu, Wu, Feng, Chang, & Li, 2008).

2.3.4 Phase inversion

If a system has two immiscible liquid-liquid phases, in this case oil and water, there are two major types of dispersions. One, where there is a continuous phase of water and the oil is dispersed in droplets. This dispersion called Oil-in-water. And another where the oil is the continuous phase with water dispersed as droplets. This dispersion called water-in-oil. The inversion of one of these dispersions to the other when there is an infinitesimal change to the systems properties is called phase inversion. The inversion point is illustrated in Figure 3.

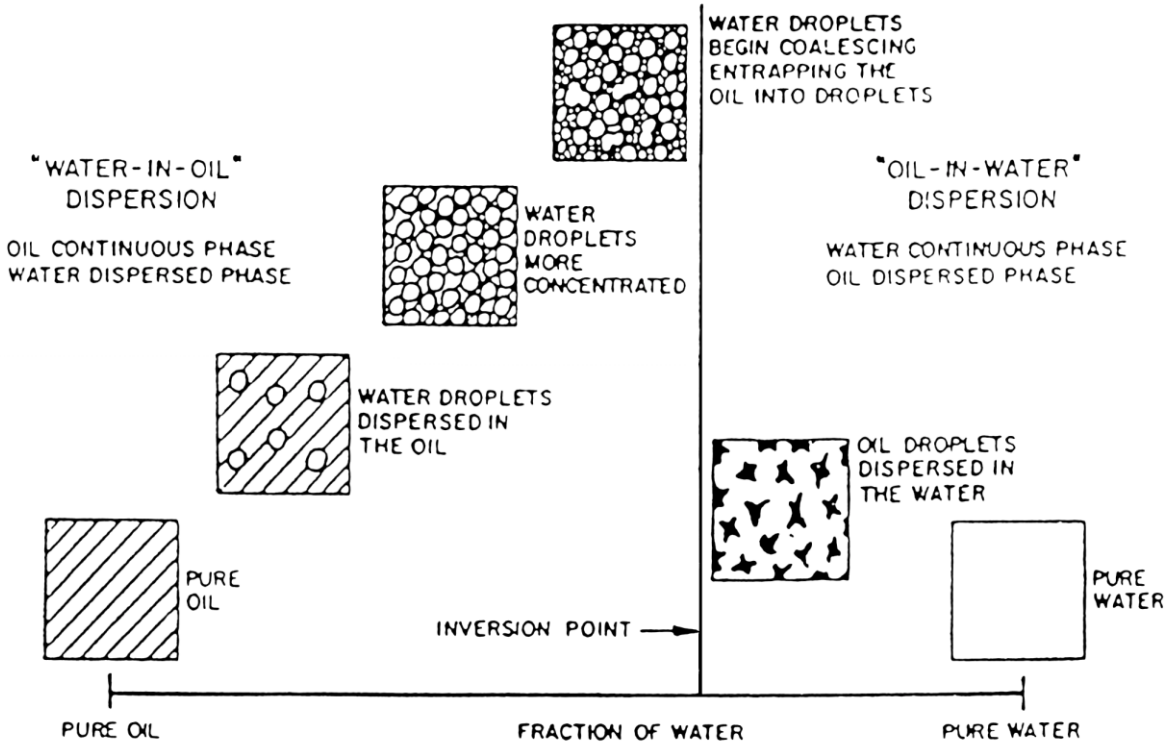

Figure 3 Illustration of oil and water dispersions and inversion point. (Arirachakaran, Oglesby, Malinowsky, Shoham, & Brill, 1989)

The closer the system is to the inversion point, there more unstable it is. Knowledge about the phase inversion point is important to effectively separate two immiscible phases since the settling time are different in oil-in-water and water-in-oil. The phase inversion is affected by liquid properties, such as viscosity, density and interfacial tension, and geometrical factors such as the material of construction, the wetting characteristics and the method of mixing.

It has been suggested that the phase inversion point will occur at the phase fraction where the apparent viscosities of the oil and the water continuous dispersions become equal. This indicated that the viscosity of the liquid-liquid mixture plays a vital part in phase inversion (Nigan, Ioannou, Rhyne, Wang, & Angeli, 2009).

3 Experimental

An experimental approach has been developed to obtain relations between the oil and water velocities in counter-current oil and water flow at inclinations between 0 and 90 degrees. The experiments investigate the effects of several different flow parameters that are believed to have an influence on the outcome. The experimental setup, which is a simple one, is constructed for the purpose of conducting these experiments and is based on visual inspection of flow patterns.

3.1 Experimental setup

The experiments were carried out using a two meter long sealed plexiglas cylinder completely filled with water and oil. Effort was put into ensuring that there was no residual air in the cylinder. The cylinder was mounted a vertical wall with a white background. The center of the cylinder was held by a rotatable arm, allowing for full rotation about its center point. The setup is illustrated in Figure 4. Specific angles between 0 and 90 degrees were measured up with a level and indicated on the background with 5 to 10 degree intervals. The experiments consisted of rotating this cylinder to a certain angle and observe the motion of its content visually. Each experiment would be recorded with a digital SLR camera, Canon EOS 60D. The video footage would then be analyzed using the video editing software Avidemux, allowing for the film to be watched frame by frame. The flow would be observed closely to establish front velocities for both oil and water. The rotation of the cylinder was done manually. A yellow color was added to the water phase to help visually distinguish it from the oil phase. To aid in determining the front position, 10 cm intervals were indicated on the cylinder itself.

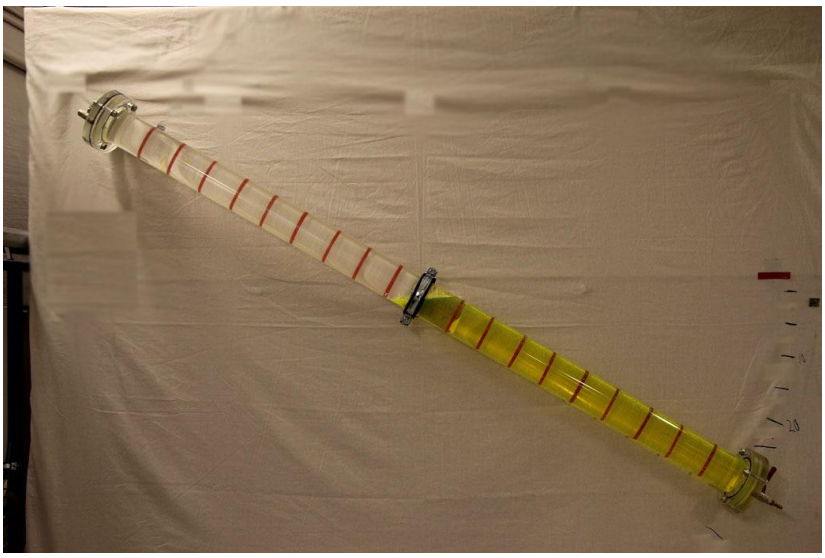

Figure 4 Overview of the experimental setup illustrated with a 90mm ID cylinder.

3.2 Method

All experiments consisted of moving the cylinder from a given start position to a final position between 0 and 90 degrees illustrated in Figure 4. It was expected that the maximum velocities would be obtained at low angles, i.e. between 10 and 30 degrees. As the low angle experiments would be the fastest ones, it was thought that experimental errors would have a

larger affect. Thus it would be beneficial to have a larger data pool in this region. Therefor a 5 degree interval was used here. For experiments with angles between 30 and 90 degrees a 10 interval was used. All experiments were repeated five times at each angle to mitigate random errors as described in the error section, chapter 3.4.

A wide range of experiments were executed using three different starting conditions, two different mineral oils as the oil phase, three different water cuts and two different inner diameter cylinders. A total of 755 experiments were conducted. These individual parameters will be described in the following sections.

3.2.1 Starting conditions

Three different types of experiments were devised, each based on different starting conditions. The purpose was to find as much useful information as possible with the simple experimental setup.

3.2.1.1 Horizontal

In these sets of experiments the cylinder was initially in a horizontal position, where the oil and water phases were completely separated and the liquids were motionless. The cylinder was then rotated to the desired angle, and the water front forming at the bottom of the pipe was tracked until full separation was obtained. A simplified illustration is presented in Figure 5.

The low angles were deemed the most interesting and a 5 degree interval was therefore used on the low angles. For angles above 30 degrees a 10 degree interval was used. After each experiment the cylinder was placed in the initial starting position and given time to settle so that the phases where again completely separated and the next experiment could commence.

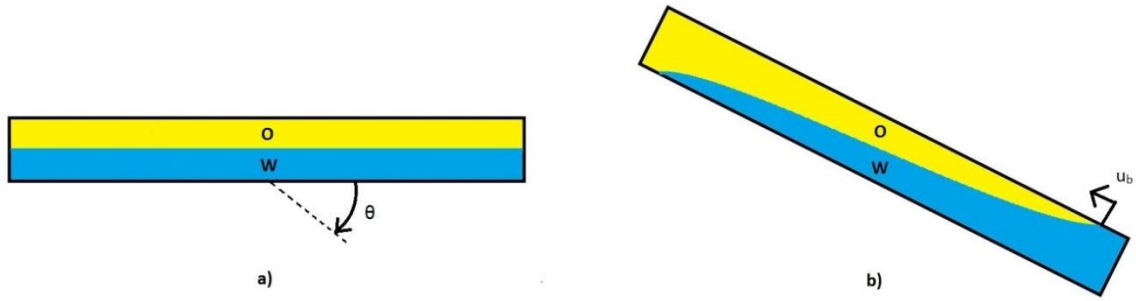

Figure 5 Illustration of *horizontal* experiments. a) Shows the initial starting conditions with the phases fully separated, b) shows the cylinder at an inclination with the fronts forming.

3.2.1.2 Mixed

These experiments were created to simulate mixed flow, i.e. counter-current dispersed phases. Mixing of the phases was obtained through a rather simple method of rotating the cylinder 180 degrees from a vertical starting point four times consecutively while allowing some time for the phases to mix, Figure 6 a). It was then placed at the desired angle, so that the end that was initially at the top is now the lowest point as shown in Figure 6 b). The mixing was done manually and time was recorded to ensure that the procedure remained as identical as possible for all experiments. As a water front developed in the bottom of the cylinder, the position of the front was measured with respect to time to establish front velocities.

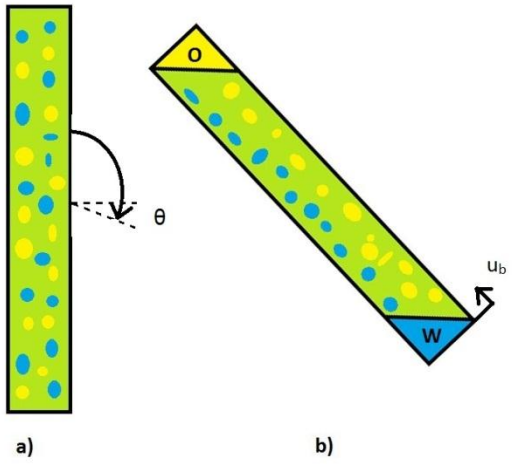

Figure 6 Illustration of the *mixed* experiments. a) Shows the initial starting condition with the phases fully mixed and b) shows the oil- and water-fronts forming.

3.2.1.3 Vertically Separated

In these experiments, the cylinder was initially in a vertical position with the oil and water phases completely separated. The cylinder was then rotated to the desired angle as shown in Figure 7 a). The experiments were divided in two phases. In the first phase, the oil- and water-fronts moving through the other phase were tracked as shown in Figure 7 b). After the fronts had reached the ends, the second phase of the experiments began where the phases separated again, Figure 7 c). In this phase, the time from when the fronts had reached the outer ends of the cylinder until full separation was recorded. By doing this, it is possible to obtain an additional data set for oil-water counter-current flow, where the phases are presumably mixed differently from the *mixed* type experiments. And although no quantifiable measure of the degree of mixing was available, it can be generally assumed that the phases will be less mixed in these experiments.

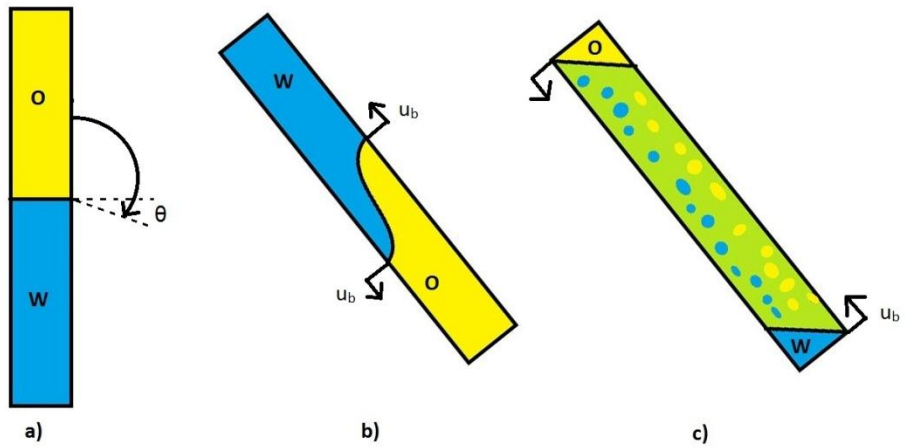

Figure 7 Illustration of the *vertically separated* experiments. a) Shows the initial starting position, b) shows the first phase of the experiments and c) shows the second phase.

3.2.2 Water cut

To investigate the effects of oil to water ratio within the cylinder, experiments were conducted for three different water cuts. The water cut in these experiments is defined as the volume fraction of water of the total liquid volume, Equation 2.2. In the initial experiments (base case), a water cut of 0.5 was used. However, experiments with 0.25 and 0.75 water cut were also performed in the 50mm ID cylinder using Exxsol D80 as the oil phase. Both *horizontal* and *mixed* experiments were conducted for all water cuts.

3.2.3 Oil types

To investigate the effects of different oil properties such as viscosity and density, experiments were conducted with two different white mineral oils as the oil phase. The oils used and their properties are listed in Table 1.

Table 1 Fluid properties[1]

Properties	**Water**	**Exxsol D80**	**Marcol 52**
Density, ρ @20°C *[kg/m³]*	998	798	825-834
Kinematic Viscosity, ν @20°C *[mm²/s]*	1	2,18	7-8
Interfacial Tension, σ *[mN/m]*		34,4	35,4

3.2.4 Pipe diameter

To investigate the effects of pipe diameter, two cylinders with different inner diameter, ID, was used. The small cylinder had an ID of 50mm and had a total volume of 3,93 liters. The large cylinder had an ID of 90mm and had a total volume of 12,72 liters. Both cylinders were

[1] Exxsol D80 and Marcol 52 properties as specified by manufacturer. Interfacial tension between oil and water phase found for Marcol 52 by (Plasencia & Nydal, 2010) and for Exxsol D80 by (Danielson, 2007).

2 meter long. The small pipe diameter was initially chosen, but experiments were extended to cover a larger diameter as well since it has been suggested that the flow patterns could vary qualitatively from small to large diameters. Experiments with *horizontal*, *mixed* and *vertically separated* were all conducted in the large cylinder. In all Large Diameter experiments Marcol 52 was used as the oil phase.

3.3 Data processing

The water front position was timed at each 10cm interval and the results were plotted in Excel according to the timer on the video. So the time of when the front was at for example xx cm from the bottom, would be denoted by t'_{xx}. The starting point of the experiments was defined as halfway between when the cylinder was in a horizontal position and the final angle.

$$t_{start} = \frac{t_0 + t_{final}}{2} \qquad \text{Equation 3.1}$$

Where t_{start} is the starting time of the experiments, t_0 is the time when the cylinder is at the 0° position and t_{final} is when the cylinder is in its final position.

Next, the actual time the for the front to travel from the bottom of the cylinder to xx cm, t_{xx}, was found by

$$t_{xx} = t'_{xx} - t_{start} \qquad \text{Equation 3.2}$$

The local front velocity, expressed in meters per second, would be found by taking

$$u_{b\,xx} = \frac{0{,}1m}{t_{xx} - t_{xx-10}} \qquad \text{Equation 3.3}$$

Where xx denotes a certain position in cm from the bottom and xx-10 denotes the previous 10cm interval.

As the front would in most cases vary along the cylinder an average front velocity is introduced. The average front velocity is defined in Equation 3.4. The distance the front has moved to reach the end is divided by the time difference between the end point, t_{end}, and the starting point, t_{start}. Each water cut yields an individual distance for the front to travel.

$$u_{b\,avg} = \frac{Distance}{t_{end} - t_{start}} \qquad \text{Equation 3.4}$$

Each experiment was always carried out five times to help improve the accuracy of the results. To estimate the uncertainties, standard deviation was found for each experiment by using

$$\sigma_S = \sqrt{\frac{1}{N-1}\sum_{i=1}^{N}(u_{bi} - \bar{u}_b)^2} \qquad \text{Equation 3.5}$$

Where σ_S represents the standard deviation, u_{bi} is the measured front velocity, $\bar{u}_b$ is the average front velocity and N is the number of experiments. The data spread displayed in the results section is found by taking two standard deviations, thus indicating that the recorded velocity is within this value with 95% certainty.

In the first phase of *vertically separated* experiments, both the oil front and the water fronts were tracked using the same definition as in Equation 3.4. Oil/water front velocity ratio, O/W, has been defined as

$$Velocity\ ratio = \frac{u_{bo\ avg}}{u_{bw\ avg}} \qquad \text{Equation 3.6}$$

Where $u_{bo\ avg}$ is the average oil front velocity and $u_{bw\ avg}$ is the average water front velocity.

In the second phase of these experiments, the average front velocity was simply found by taking the time between the fronts had reached the ends of the cylinder until full separation was obtained again. Calculated by the following expression

$$u_{b\ avg} = \frac{Distance}{t_{sep} - \frac{t_{o,e}+t_{w,e}}{2}} \qquad \text{Equation 3.7}$$

Where t_{sep} denotes the time for full separation, $t_{o,e}$ denotes the time when the oil front had reached the end of the cylinder and $t_{w,e}$ denotes the time when the water front had reached the end of the cylinder.

3.4 Sources of error

Since the experiments are of such a simple method, it is important to identify and quantify all sources of error. In this section attempts have been made to do so and to describe how certain errors were mitigated during the experimental process. Also, this section can be helpful as to how to process the results when drawing conclusions and to identify what factors can be improved in future experiments.

3.4.1 Starting conditions

Due to the experimental setup, the pipe was always managed manually and there may have been some inaccuracy in placing the pipe at the desired angle. Particularly in the *horizontal* experiments this may have had a large impact, because even a small degree of inaccuracy in the starting position would lead to a significant difference in the local holdup at the outer positions of the cylinder.

The final position of the cylinder would also sometimes be inaccurate, due to the fact that it was moved quickly to minimize the time spent in motion. The cylinder angle was continuously measured with a level during experiments and this revealed that the error was very rarely greater than one degree.

The rotational speed of the cylinder during the mixing period may also differ between the experiments since the rotation was done manually. This may have led to differences in the initial motion of the fluid during the start of the experiments.

Another error related to starting conditions is that it takes a certain amount of time to put the cylinder in a desired position. The oil and water in the cylinder will continuously be in motion while the cylinder is being turned around. If the cylinder is being set at for example 80°, the water phase will start to move towards the bottom end as soon as the cylinder has passed the horizontal position of 0°. This means what happens during the time the cylinder is at the horizontal position until its final position will have to be taken into account. This was the reason for defining the starting point as described in Equation 3.1.

3.4.2 Degree of mixing

The degree of mixing in the m*ixed* experiments would vary greatly between different types of experiments, such as changing water cut, cylinder size and type of oil used. Especially for the 0.75 water cut experiments the degree of mixing was very low compared to other experiments, there was still a very significant continuous water phase during these experiments. The mixing method was kept constant, with five 180° rotations before the cylinder was set into position so that the degree of mixing would remain constant within each set of experiments. However, this error proved it more difficult to relate for example a 0.75 water cut experiment to a 0.5 water cut experiment.

Another issue related to this was that the contents would not be uniformly mixed throughout the cylinder at the start of experiments. For example; the bottom end of the cylinder would have a higher water concentration than the rest of it. This could be the reason for the very quick water front buildup that was observed during the initial phase of the experiments. As there was no sufficient way to quantify the degree of mixing, this was merely described visually and the effects of this needs to be discussed.

3.4.3 Front tracking

Since the water and oil fronts were tracked visually, determining the front position proved very difficult at times. The readings would naturally be subject to some subjectivity as the actual fronts were not always clearly defined. The front would change appearance and behavior, depending on the flow regime and the degree of mixing. Photos have been included in the results section to illustrate some of the difficulties associated with visual front tracking. In attempt to decrease the level of subjectivity, the readings would often be done individually and then comparing the results. Also, repeating each experiment five times was helpful in mitigating the extent of these errors. The magnitude of this type of error was highly dependent on the type of experiment and the angle. In general it was easier to track fronts at high angle experiments, due to the slow movement and the fact that the front was more clearly defined.

3.4.4 Transferring effects

Every experiment may have impacts on the next one. At least two such effects were observed during experiments. During experiments where bubbles formed, those would often remain stable for a long time, especially for *mixed* experiments at high inclinations. Using Exxsol D80 as the oil phase, bubbles were observed to remain in the cylinder for several days. Sometimes a thin water film was observed on the cylinder inner wall in parts of the oil phase. Therefore it was not possible to always have the exact same starting conditions since it would depend on the previous experiments. The effects of both of these occurrences have not been

thoroughly investigated, so the impacts on the experiments are unknown. Whenever such behavior was observed in the cylinder, appropriate measures were taken to mitigate the effects. This mainly included giving some time for the bubbles to settle and tilting the cylinder so that the settling would speed up.

4 Results

This section includes results from all experiments that were performed, totaling 755 experiments, divided into 13 different categories as shown in Table 2. The obtained average front velocities are first represented graphically, going through each experimental category individually. The graphs in this section are made so that each individual data point represents the five repetitions of each experiment. The spread of data is included in the graphs with dotted lines and represents two standard deviations defined by Equation 3.5. The results are also included in Appendix A. Next, there is a section that covers local front velocity profiles at 90 degree inclination. Finally some visual observations are included with illustrations to provide an overview of the observed flow patterns.

The oil front was not tracked for *mixed* and *horizontal* experiments due to it generally being quite difficult to track. This is described in detail in section 4.6.6.

Table 2 Overview of experiments

Experiments	Diameter	Oil phase	Water cut	Starting conditions	Colour Code
Base case	50mm	Exxsol D80	0.5	*Horizontal*	
				Mixed	
				Vertically separated	
Water cut	50 mm	Exxsol D80	0.25	*Horizontal*	
				Mixed	
		Exxsol D80	0.75	*Horizontal*	
				Mixed	
Marcol 52	50mm	Marcol 52	0.5	*Horizontal*	
				Mixed	
				Vertically separated	
Large Diameter	90mm	Marcol 52	0.5	*Horizontal*	
				Mixed	
				Vertically separated	

4.1 Base Case

The initial sets of experiments were conducted using Exxsol D80 with a 0.5 water cut and a 50mm ID cylinder. Both *horizontal*, *mixed* and *vertically separated* experiments were conducted with these conditions.

4.1.1 Horizontal

A set of experiments with *horizontal* starting conditions was conducted with Exxsol D80 as the oil phase with a 0.5 water cut and in a 50mm ID cylinder. Figure 8 shows the average water front velocities for cylinder inclinations between 5° and 90° from the horizontal. The dotted line indicates the data spread in the experiments. It is evident that the maximum front velocity is found in the interval between 10° and 30° and reaches about 0.14 to 0.19 m/s, but the exact inclination that yields the highest velocity is not possible to determine. It is noteworthy that the flow in the cylinder remained separated at the low angles, but the flow was dominated by waves. At roughly 20°, the waves started to break up and the flow was increasingly more chaotic with increasing angles. At higher inclinations, the flow became more dispersed, even though the channeling effect was clearly visible up until 90°. At

inclinations above 30°, there is a steady decline in the average water front velocity until it reaches its minimum point of roughly 0.04m/s at 90°. The spread of data was generally larger at lower angles due to the faster movement.

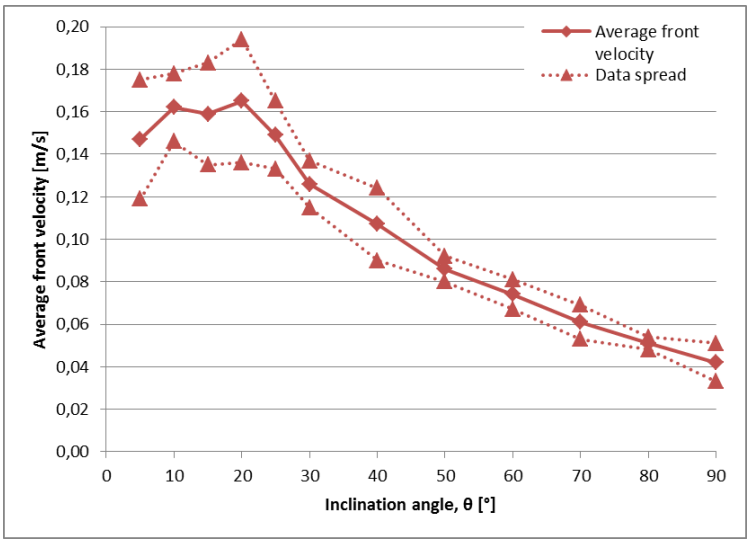

Figure 8 Average water front velocities for Base Case *horizontal* experiments.

4.1.2 Mixed

A set of experiments with *mixed* starting conditions was conducted with Exxsol D80 as the oil phase with a 0.5 water cut and in a 50mm ID cylinder. Figure 9 shows the measured water front velocities for cylinder inclinations between 10° and 90°, with data spread displayed by the dotted lines. It is evident that a maximum front velocity of roughly 0.07 to 0.09m/s is found in the low angle region between 10° and 25° inclination. At inclinations above 20° there is a decline in the average water front velocity until it reaches its minimum point of roughly 0.02m/s at a vertical position. At low angles, the flow was observed to separate quickly in the vertical direction, but this effect diminished as the cylinder angle approached 90°.

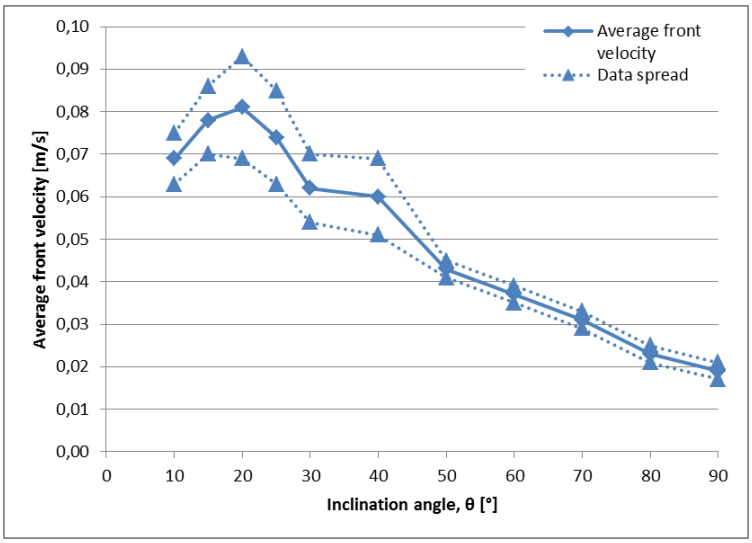

Figure 9 Average water front velocities for Base Case *mixed* experiments.

4.1.3 Vertically separated

4.1.3.1 First phase

A set of experiments with *vertically separated* starting conditions was conducted with Exxsol D80 as the oil phase with a 0.5 water cut and in a 50mm ID cylinder. Figure 10 illustrates the average oil and water front velocities at inclinations between 5 and 90 degrees during the first phase of these experiments. From the figure it is evident that the water phase flows at a higher velocity compared to the oil phase, but the water phase also has a higher uncertainty due to a more wavy flow. The highest front velocities are found in the region between roughly 20° and 50° inclination.

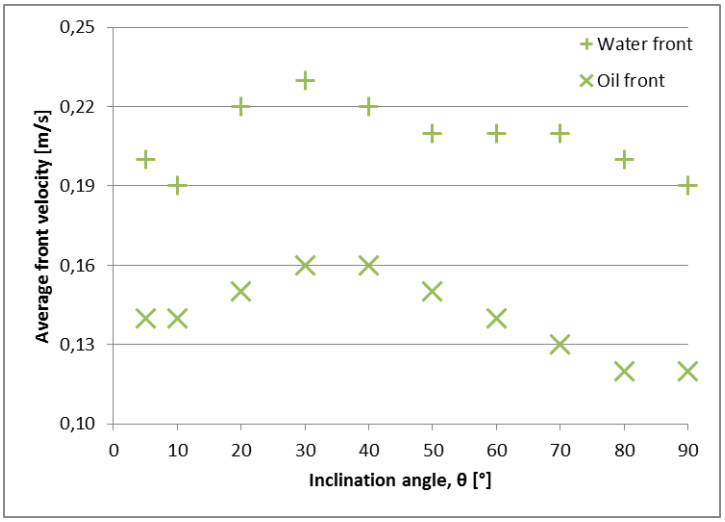

Figure 10 Average water and oil front velocities during the first phase of Base Case *vertically separated* experiments.

4.1.3.2 Second phase

In Figure 11the separation time for the second phase of these experiments is shown for angles between 5 and 90 degrees. At low angles the separation time is short but is steadily increasing from about 30 degrees and up to 90 degrees. The phases were fairly separated during the entire separation process at low angles until roughly 30 degrees, while becoming increasingly dispersed as the inclination increased. The point of full separation became increasingly unclear at higher angles because more bubbles were being formed and the flow was more obscure.

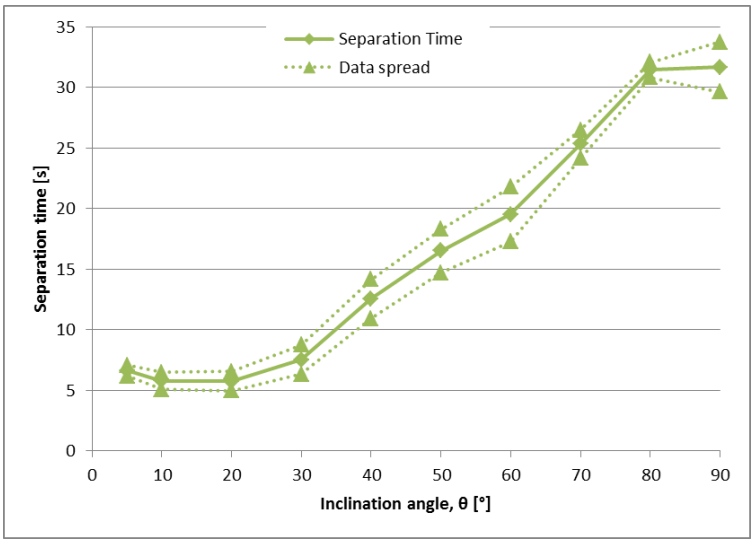

Figure 11 Separation time during the second phase of Base Case *vertically separated* experiments.

4.2 Water Cut

This section covers the results from experiments using different water cuts for both *horizontal* and *mixed* type experiments.

4.2.1 Water cut 0.25

4.2.1.1 Horizontal

A set of experiments with *horizontal* starting conditions was conducted with Exxsol D80 as the oil phase with a 0.25 water cut and in a 50mm ID cylinder. Figure 12 shows the measured water front velocities for cylinder inclinations between 5° and 90°. It is evident that the maximum front velocity is found between roughly 10 and 30 degrees inclination. At the very lowest inclinations, the water and oil phase would flow completely separated with little to no wave formation. At 15°, these waves would occasionally become large enough to form some small droplets due to break off. This behavior was further enhanced as the inclination increased and at roughly 40° inclination, a mixed zone started to form above the water front. The average water front velocity was found to steadily decrease as inclinations exceeded 40 degrees.

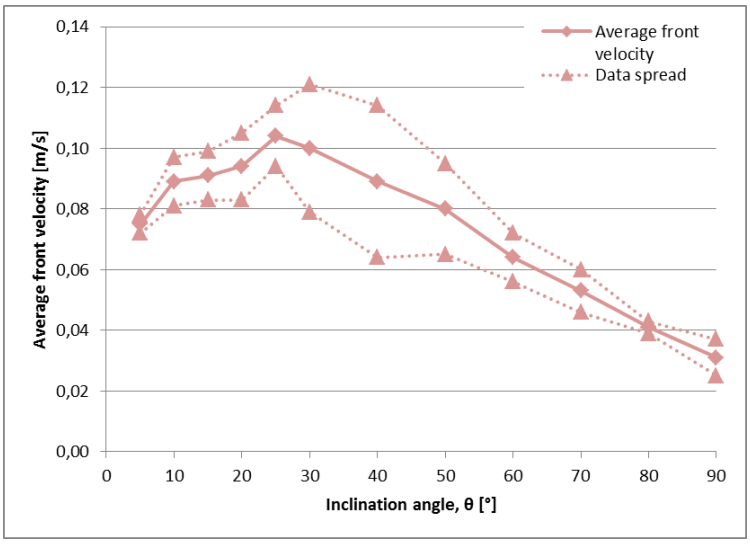

Figure 12 Average front velocities for Water Cut 0.25 *horizontal* experiments.

4.2.1.2 Mixed

A set of experiments with *mixed* starting conditions was conducted with Exxsol D80 as the oil phase with a 0.25 water cut and in a 50mm ID cylinder. Figure 13 shows the measured water front velocities for cylinder inclinations between 5° and 90°. It is evident that the maximum front velocity reaching almost 0.04m/s is found at inclinations between 10° and 30°. After this point, the velocity steady decreases towards a minimum of roughly 0.014m/s at 90° inclination. At low angles, a large continuous oil phase appeared within seconds of the start due to the water tending to flow along the bottom of the cylinder. At higher inclinations, as the channeling effect diminished, the phases remained more and more dispersed in each other. The experiments were also generally characterized by rapid accumulation of water in the initial phase, continuously slowing down until the separation was complete. This behavior was observed at all inclinations.

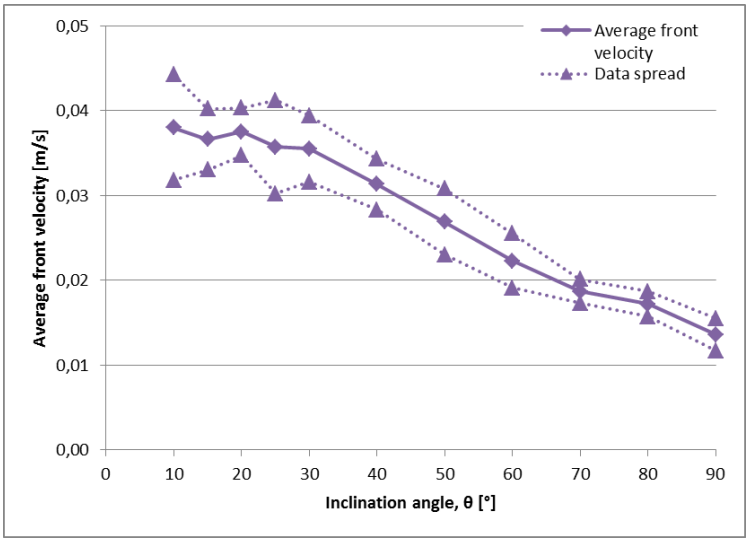

Figure 13 Average front velocities for Water Cut 0.25 *mixed* experiments.

4.2.2 Water cut 0.75

4.2.2.1 Horizontal

A set of experiments with *horizontal* starting conditions was conducted with Exxsol D80 as the oil phase with a 0.75 water cut and in a 50mm ID cylinder. Figure 14 shows the measured water front velocities for cylinder inclinations from 5° to 90°. It is evident that the maximum front velocity is found in inclinations between 5 and 25 degrees. At low angles, the phases remained completely separated, although a higher degree of wave formation was observed compared to the 0.25 water cut experiments. Wave breakups and bubble formation were initially observed at 15° to a small extent, and this behavior was enhanced at higher inclinations. At roughly 40° a mixed zone started to form between the continuous oil and water phases and the extent of this zone increased as the inclination increased.

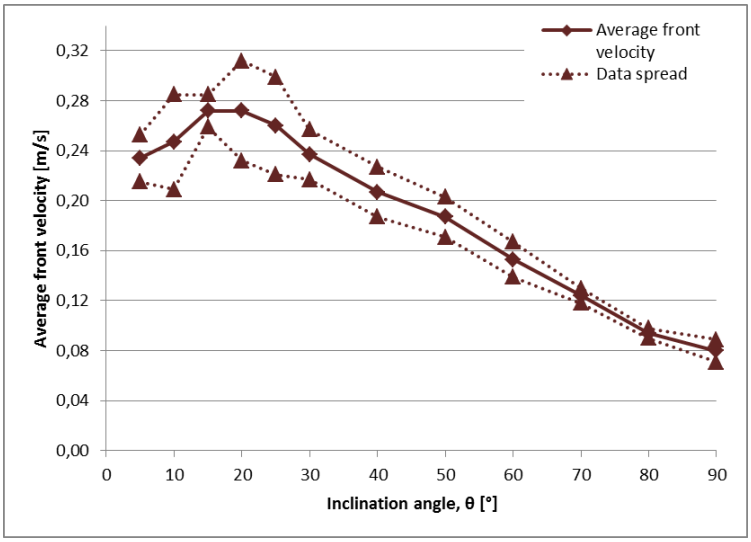

Figure 14 Average front velocities for Water Cut 0.75 *horizontal* experiments.

4.2.2.2 Mixed

A set of experiments with *mixed* starting conditions was conducted with Exxsol D80 as the oil phase with a 0.75 water cut and in a 50mm ID cylinder. Figure 15 shows the measured water front velocities for cylinder inclinations between 5° and 90°. It is clear that the maximum velocity of roughly 0.20 to 0.25m/s is found between 15 and 40 degrees inclination. Noteworthy for these experiments is that while a mixed zone was successfully created, the entire contents of the cylinder were not mixed and there was a large continuous water phase surrounding the mixed phase. At low angles, this mixed phase would flow along the top of the pipe consisting of a continuous oil phase full of bubbles containing water and oil, continuously separating in the vertical direction. As inclinations increased, the mixed zone would flow faster towards the top, while the separation in the direction normal to the cylinder would decrease. At inclinations from 40° and up, the mixed zone covered almost the entire cylinder and the signs of channelization became less and less obvious.

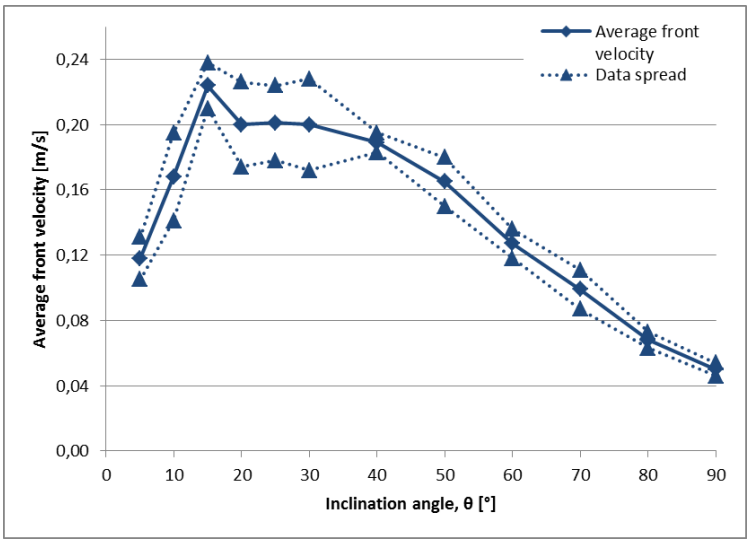

Figure 15 Average front velocities for Water Cut 0.75 *mixed* experiments.

4.3 Marcol 52

This section covers results from experiments using a different white mineral oil, Marcol 52, as the oil phase. Experiments were performed for *horizontal*, *mixed* and *vertically separated* starting conditions.

4.3.1 Horizontal

A set of experiments with *horizontal* starting conditions was conducted with Marcol 52 as the oil phase with a 0.5 water cut and in a 50mm ID cylinder. Figure 16 shows the measured water front velocities for cylinder inclinations from 5° to 90°. It is evident that the maximum front velocity is found in at inclinations between 15° and 30°, however the uncertainties are so significant that the actual maximum point is not possible to determine. It is noteworthy that the flow in the cylinder remained separated at the low angles, but the flow was dominated by waves. At roughly 20°, the waves started to break up and the flow was increasingly more chaotic with increasing angles. At higher inclinations, the flow became more dispersed, even though the channeling effect was clearly visible up until 90°. At inclinations above 30°, there is a steady decline in the average water front velocity until it reaches its minimum point at 90°.

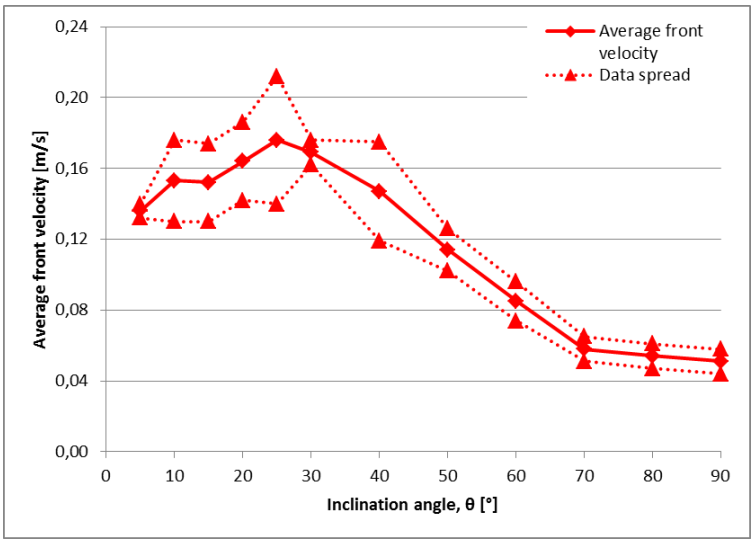

Figure 16 Average front velocities for Marcol 52 *horizontal* experiments.

4.3.2 Mixed

A set of experiments with *mixed* starting conditions was conducted with Marcol 52 as the oil phase with a 0.5 water cut and in a 50mm ID cylinder. Figure 17 shows the measured water front velocities for cylinder inclinations from 5° to 90°. The maximum front velocity of roughly 0.08 m/s is found at inclinations between 10 and 25 degrees. At inclinations above 40°, there is a steady decline in the average water front velocity until it reaches its minimum point at 90°. At low angles, the flow was observed to separate quickly in the vertical direction, but this effect diminished as the cylinder angle approached 90°.

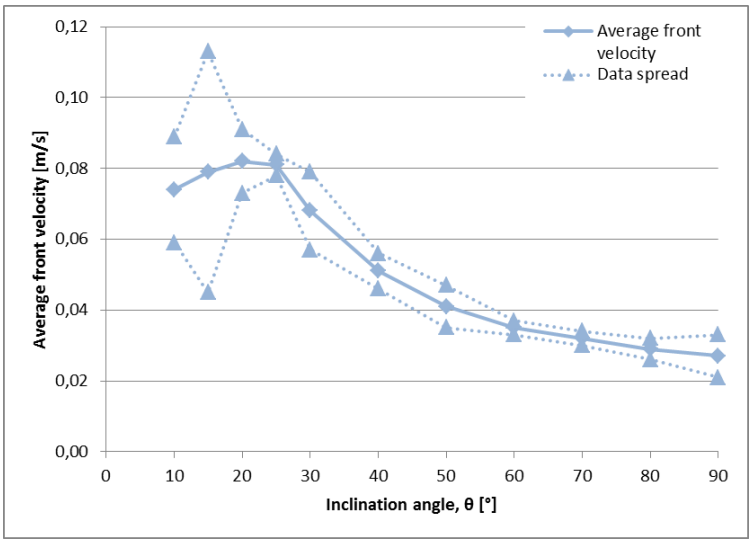

Figure 17 Average front velocities for Marcol 52 *mixed* experiments.

4.3.3 Vertically Separated

4.3.3.1 First phase

A set of experiments with *vertically separated* starting conditions was conducted with Marcol 52 as the oil phase with a 0.5 water cut and in a 50mm ID cylinder. In Figure 18, the average water and oil front velocities are presented. In these experiments the water and oil fronts have

relatively similar velocities for all inclinations. The waterfront is seen to move at a somewhat higher velocity than the oil front at inclinations above 50 degrees. The highest velocities are found in the region between 15 and 50 degrees inclination.

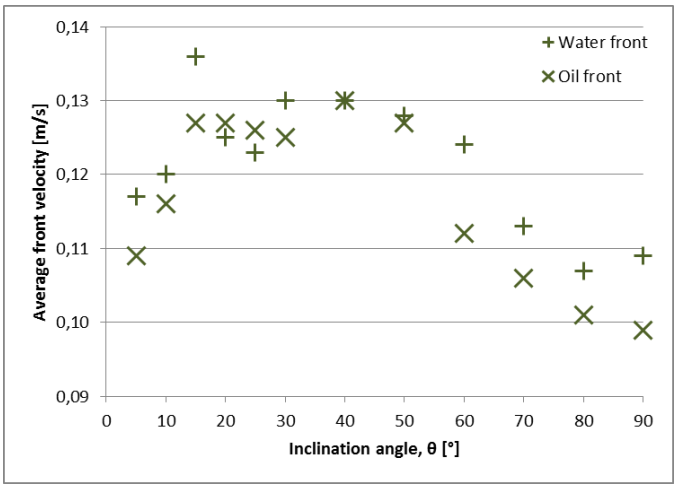

Figure 18 Average water and oil front velocities during the first phase of Marcol 52 *vertically separated* experiments.

4.3.3.2 Second phase

Figure 19 illustrates the measured separation time in the *vertically separated* experiments using Marcol 52 and a 0.5 water cut in a 50mm ID cylinder. The separation time remains low and almost constant at low inclinations up until about 30 degrees. After this point, the separation time steadily increases with higher inclinations until the maximum time at 90 degrees.

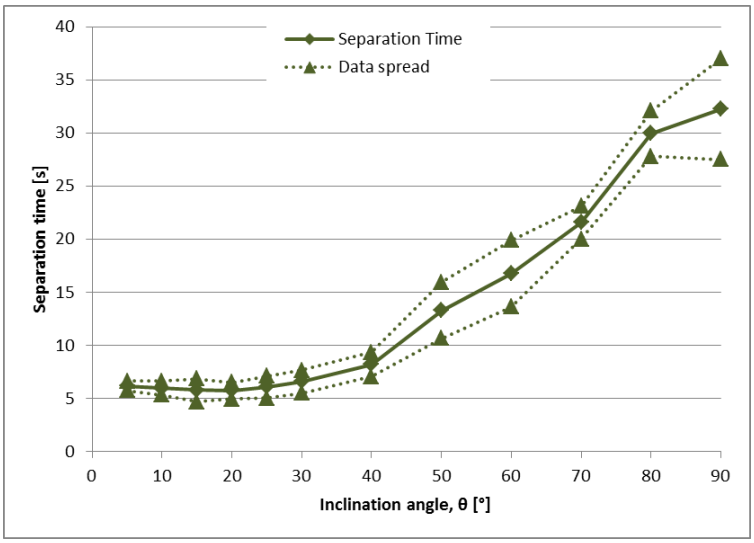

Figure 19 Separation time for Marcol 52 *vertically separated* experiments.

4.4 Large Diameter

This section covers the results from experiments using a larger cylinder inner diameter. Experiments with *horizontal*, *mixed* and *vertically separated* starting conditions are included.

4.4.1 Horizontal

A set of experiments with *horizontal* starting conditions was conducted with Marcol 52 as the oil phase with a 0.5 water cut and in a 90mm ID cylinder. Figure 20 shows the measured water front velocities for cylinder inclinations between 5° and 90°. The maximum velocity is found at low angles, between 15 and 30 degrees inclination. The observed flow patterns were similar to those in the small diameter cylinder. It was generally found to be easier to follow the water front in the large cylinder, resulting in less spread of the data.

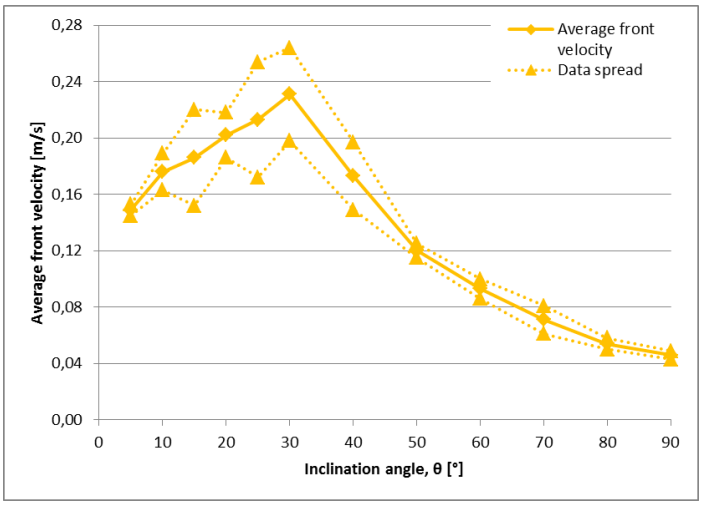

Figure 20 Average front velocities for Large Diameter *horizontal* experiments.

4.4.2 Mixed

A set of experiments with *mixed* starting conditions was conducted with Marcol 52 as the oil phase with a 0.5 water cut and in a 90mm ID cylinder. Figure 21 shows the measured water front velocities for cylinder inclinations between 5° and 90°. The maximum velocity is found to be between 5 and 30 degrees inclination. The spread of data in these experiments was high compared to the *horizontal* ones due to the large amount of bubbles in the flow. As the inclination increased, the front became much more distinct and slow moving, making it easier to track.

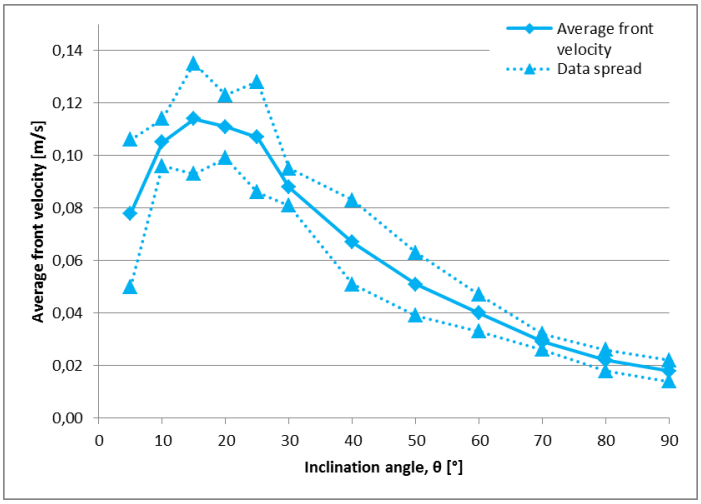

Figure 21 Average front velocities for Large Diameter *mixed* experiments.

4.4.3 Vertically Separated

4.4.3.1 First Phase

A set of experiments with *vertically separated* starting conditions was conducted with Marcol 52 as the oil phase with a 0.5 water cut and in a 90mm ID cylinder. In Figure 22, the average water and oil front velocities are presented. The same pattern is observed as for the same type of experiments with the same oil in the 50mm ID cylinder, except that there is a slight clearer tendency towards the oil front moving slower than the water phase. The highest velocities are found in the region between 20 and 60 degrees inclination.

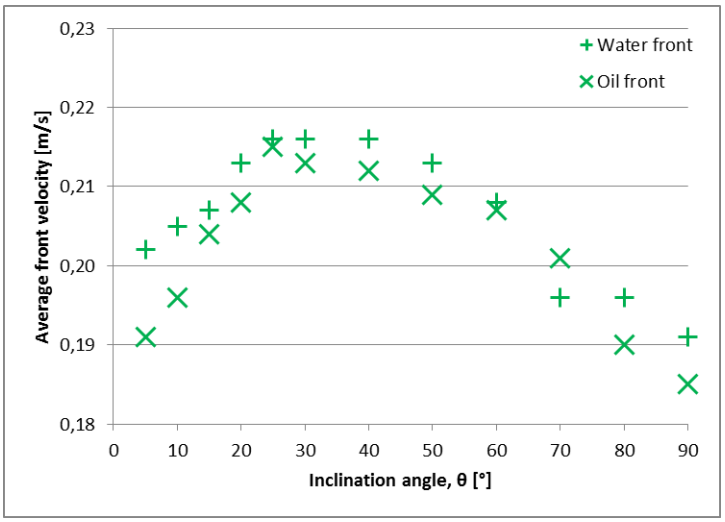

Figure 22 Average water and oil front velocities during the first phase of Large Diameter *vertically separated* experiments.

4.4.3.2 Second Phase

The measured separation time in the second phase of *vertically separated* experiments using Marcol 52, a 0.5 water cut and in a 90mm ID cylinder are displayed in Figure 23. The separation time remains low and rather constant at low angles up until 30 degrees. At inclinations above this point, the separation time is observed to steadily increase with increasing inclination until reaching its maximum point at 90 degrees.

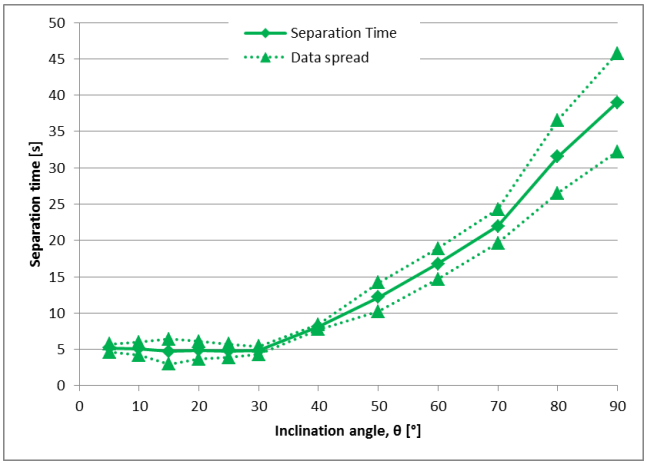

Figure 23 Separation time for Large Diameter *vertically separated* experiments.

4.5 Local front velocities

Even though the results in the previous section are based on average front velocities as calculated from Equation 3.4, attempts were made to establish local front velocity profiles. This section presents an overview of local front velocity measurements during both *horizontal* and *mixed* experiments calculated by Equation 3.3. The simple setup used in this study made it quite difficult to establish local front velocity profiles with a decent degree of certainty. In most cases the front was moving rather quickly and was not well defined as is shown in Section 4.6 where photos of the front are included. Especially at low angles where the front was wave dominated and was moving very quickly, the uncertainties were so high that attempts at establishing local front profiles in those cases were abandoned. This was also the case for experiments with alternative water cuts; for 0.25 water cut the front did not travel far enough to even establish a meaningful velocity profile as there were too few data points. For 0.75 water cut, the front was moving so fast that the uncertainties became very large. However, the local front velocity was observed to vary significantly throughout experiments and it was deemed important to put some focus on this as it impacts the applicability of the results of this research. This section gives an overview of local front velocity profiles from *horizontal* and *mixed* experiments at 90° inclination since these were the most reliable results obtained. The results are based on the interval from 10cm to 90cm since it is not possible to define a front at 0cm and the 100cm mark was generally not reached due to bubble formation.

4.5.1 Horizontal

Front tracking in *horizontal* experiments is characterized by a continuously changing front by visual appearance. At low angles of inclination, the movement is dominated by waves and the front alternates between moving slow and fast. This makes the results at low angles seem rather random and the observed variation between two similar experiments was very large. At 90 degrees inclination, the front was cluttered with bubbles, but moving more slowly and similar experiments gave somewhat similar results with markedly less variation.

Figures 24 through 26 show local front velocity profiles obtained for *horizontal* experiments. The results are quite similar for Base Case, Marcol 52 and Large Diameter type experiments with a high front velocity initially, decelerating as the experiment goes on. The measured velocities do not show significant variation in magnitude for different oils or pipe diameters except perhaps for the first data point. There is quite a significant difference between the velocities found at 20cm compared to that at 90cm in all cases, the first being several times as high as the latter. The measured velocity is continuously changing throughout the experiment and does not remain constant at any interval. The water that is originally near the bottom has a rather short path, while the water at the top of the cylinder must pass all the oil that is flowing upwards, thus experiencing much more friction. The same pattern was observed at lower inclinations as well, but to a less extent as there were generally less bubbles in the flow with decreasing inclination.

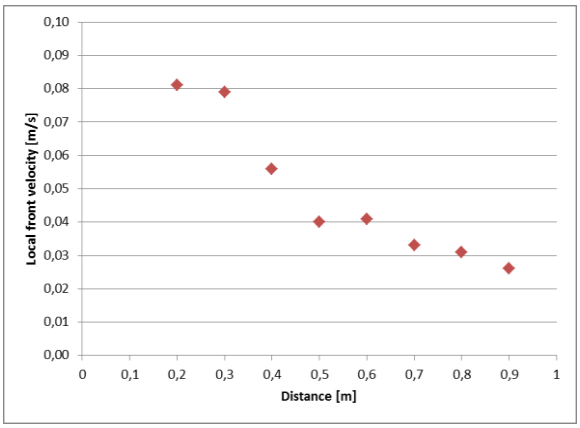

Figure 24 Local front velocity profile for Base Case *horizontal* experiments at 90° inclination.

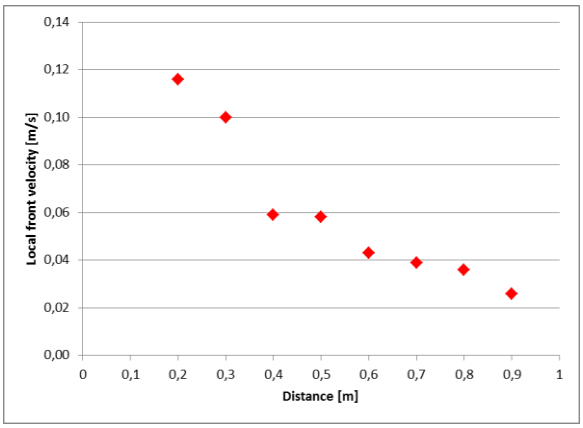

Figure 25 Local front velocity profile for Marcol 52 *horizontal* experiments at 90° inclination.

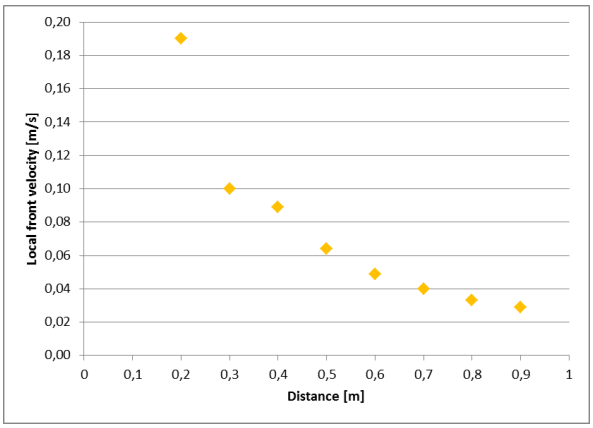

Figure 26 Local front velocity profile for Large Diameter *horizontal* experiments at 90° inclination.

4.5.2 Mixed

Front tracking during *mixed* experiments saw some of the same problems that were encountered in *horizontal* experiments. At low inclinations, the front was not well defined and observations for two similar experiments would yield very different results making it too unreliable. Experiments at high inclinations proved more suitable for more exact front tracking and results at 90° inclination were found to be the most reliable.

Figure 27 shows the development of the water front velocity throughout the cylinder for Base Case experiments at 90° inclination. The front velocity is seen to be relatively high, roughly 0.03m/s initially, then quickly dropping off to about 0.015m/s at 30cm. The velocity then remains at this level for another 20cm, after this point it slowly increases towards another maximum of 0.025m/s at 80cm. Finally the front velocity drops off towards the end. It was observed that the content was not uniformly mixed and there was a small continuous water phase present at the bottom of the cylinder at the start of experiments. This is likely to be the reason why the observed velocity was so high initially. The flow between 30cm and 80cm is characterized as quite stable, but is seen to be accelerating somewhat during this interval. From 80cm and upwards, the flow was stagnating and the front speed approached zero before 100cm was reached due to some part of the bubbles and foam being stable over a longer period of time. The behavior of acceleration up until 70-90 cm and then rapidly decreasing towards the last 10-30cm was observed at all inclinations.

Figure 28 shows the local waterfront velocity at 90 degree inclination with Marcol 52 as the oil phase. The same pattern that was observed for Exxsol D80 was observed here. The measured velocity was initially very high, due to a continuous water phase already having formed at the bottom of the cylinder. This water phase was generally larger in the case of Marcol 52 compared to Exxsol D80, indicating that the content was somewhat less mixed.

A distinct difference between the large and the small cylinder was observed. In the large diameter cylinder, Figure 29, a higher degree of mixing appeared to be obtained using the same mixing method. No continuous water phase was observed in the bottom of the cylinder at the start of these experiments contrary to the previous ones. The initial velocity was still high and there may still have been a high concentration of water at the bottom of the cylinder at the start of experiments that was not distinguishable visually. A closer examination of the local water front velocity at 90 degrees inclination reveals the same patterns that were observed for both Exxsol D80 and Marcol 52 in the smaller cylinder.

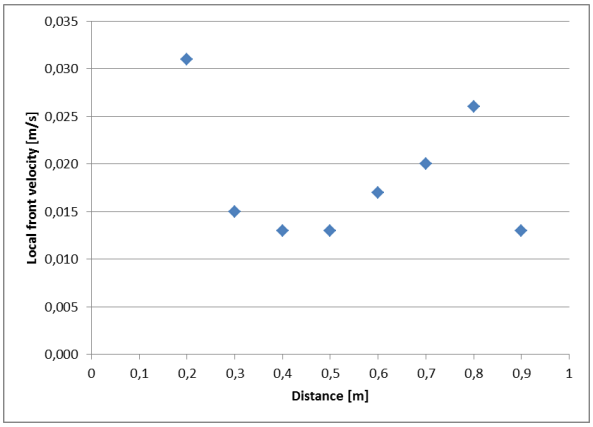

Figure 27 Local front velocity profile for Base Case *mixed* experiments at 90° inclination.

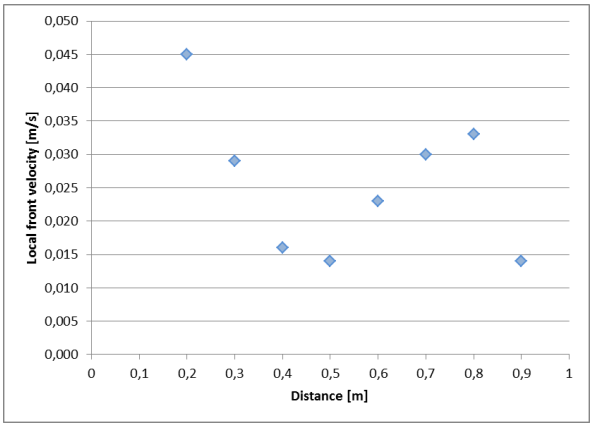

Figure 28 Local front velocity profile for Marcol 52 *mixed* experiments at 90° inclination.

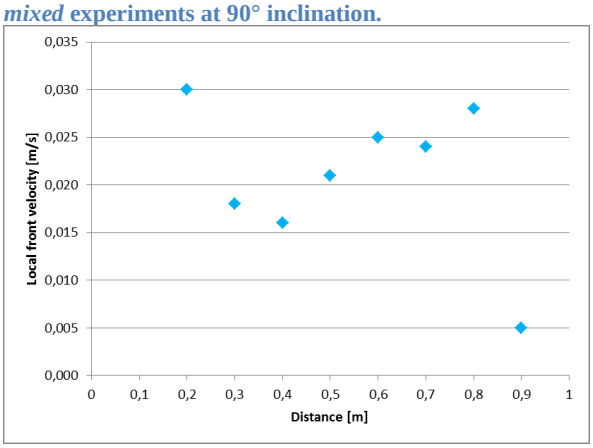

Figure 29 Local front velocity profile for Large Diameter *mixed* experiments at 90° inclination.

4.6 Flow Patterns

This section contains several photos of different flow patterns that were observed during the experiments. Photo series illustrating both water and oil front propagation for all three starting conditions. Flow patterns were found to remain very similar for Exxsol D80 and for Marcol 52, the main difference being somewhat increased bubble formation in the case of Exxsol D80. The photos included in this section are all taken with Marcol 52 as the oil phase. There

were no distinct changes in flow patterns between the two cylinder sizes that were used. However, the large cylinder did prove to offer better visibility of the flow and one photo series is included to illustrate this difference. The photos are not taken at constant intervals and are merely included to illustrate flow patterns. The observed flow patterns can mainly be described by the following flow regimes; stratified for low inclinations, three-layer and dispersed flow with channelization for intermittent inclinations and fully dispersed flow for vertical inclinations. Stratified flow is defined by a stable interface, sometimes quite wavy, but with no breakoff or bubbles in the flow and is only observed for *horizontal* experiments and in the first phase of *vertically separated* experiments. Three-layer flow is defined by continuous oil and water phases at the top and the bottom of the cylinder cross-section with a foamy/bubbly layer in between and is mainly observed in *mixed* experiments. Dispersed flow with channelization can be described as both phases being dispersed into bubbles and no continuous phase is evident, but the bulk flow of water happens along the bottom side of the cylinder and vice versa for the oil phase. Fully dispersed flow is a chaotic flow pattern that is mainly observed at vertical inclinations for all types of experiments. These flow patterns are based strictly on visual appearances.

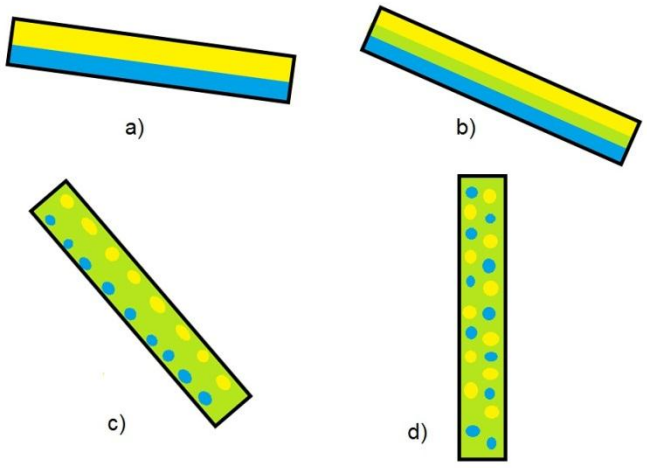

Figure 30 Illustration of observed flow patterns, a) separated flow b) three layer flow c) dispersed flow with channelization d) fully dispersed flow.

4.6.1 Horizontal

4.6.1.1 Water front

Figure 31 illustrate the progression of the water front during *horizontal* experiments at angles 10, 30, 60 and 90 degrees. At a 10 degree inclination, Figure 31 a), the flow in the cylinder is wave dominated and the phases remain separated with few bubbles forming. The front is not well defined at this inclination and it is evident that visual front tracking involves quite some subjectivity. At 30 degrees inclination as shown in Figure 31 b), the interface between the two phases is cluttered with bubbles and the flow is generally more chaotic, however two continuous phases are still present. The front was not moving at a constant speed, water was observed to fill the bottom pipe rather quickly at first and then slowing down as mostly bubbles remained. At 60 degrees, the phases are much more dispersed in each other, effectively creating a mixed zone between the continuous oil and water phases. The bulk flow of oil is still along the top side of the cylinder and along the bottom for the water phase.

Finally at 90 degrees, no obvious signs of channelization are evident and the zone above the water front is mixed and dominated by small bubbles.

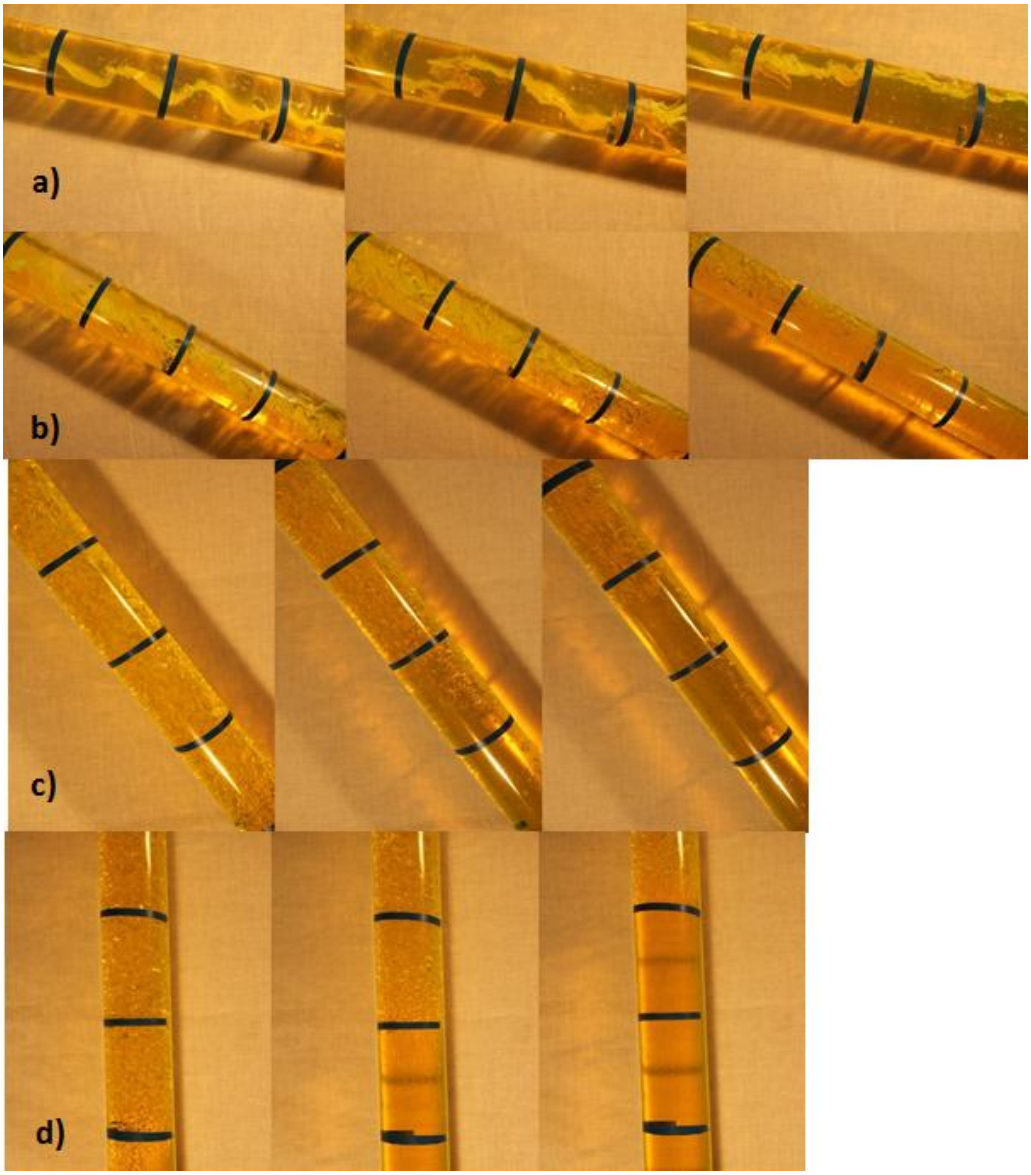

Figure 31 Photo series displaying the water front moving upwards during *horizontal* experiments in a 50mm ID cylinder at a) 10 degrees b) 30 degrees c) 60 degrees and d)90 degrees inclination.

4.6.1.2 Oil front

Figure 32 show the progression of the oil front in the cylinder. The same type of flow pattern is observed at the oil front compared to the waterfront, but at high inclinations the oil front is generally less defined due to the large amount of bubbles, thus making it more difficult to track visually. For this reason, emphasis was put onto tracking of the water front rather than tracking both fronts.

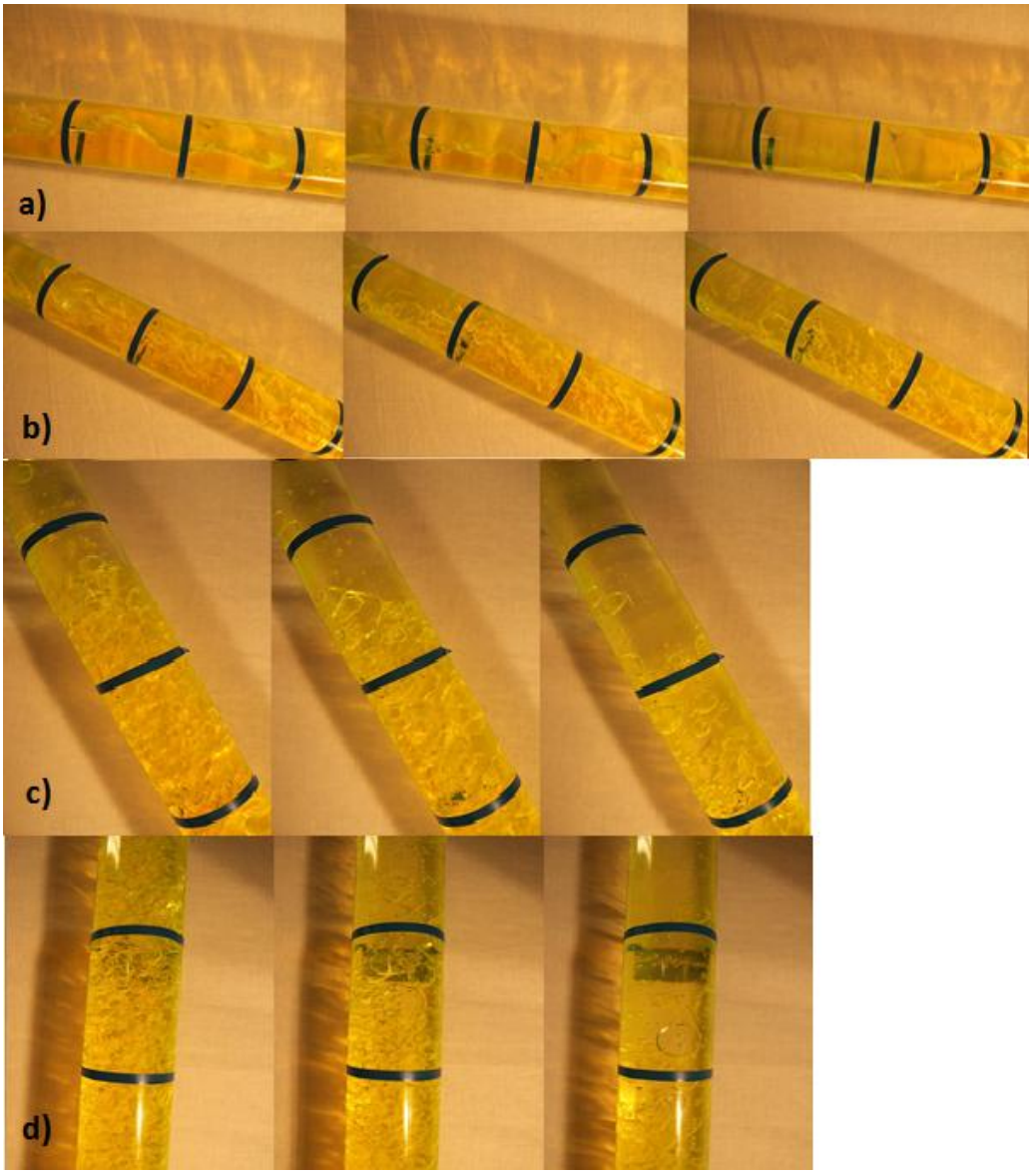

Figure 32 Photo series displaying the oil front moving downwards during *horizontal* experiments in a 50mm ID cylinder at a) 10 degrees b) 30 degrees c) 60 degrees and d)90 degrees inclination.

4.6.2 Mixed

4.6.2.1 Water front

Figure 33 displays the water front progression in the *mixed* experiments. At low inclinations the oil and water in the mixed zone separates fast in the vertical direction, thus the mixed zone experiences a transition from very dispersed to a three layer zone. This is characterized by a continuous water phase at the bottom and a continuous oil phase at the top, with a phase consisting of dispersed oil and water in the middle. At higher inclinations this is not as evident as the continuous phases diminish. The waterfront could be difficult to identify especially at low inclinations due to a tail of bubbles. At inclinations closer to vertical position, the front became more defined.

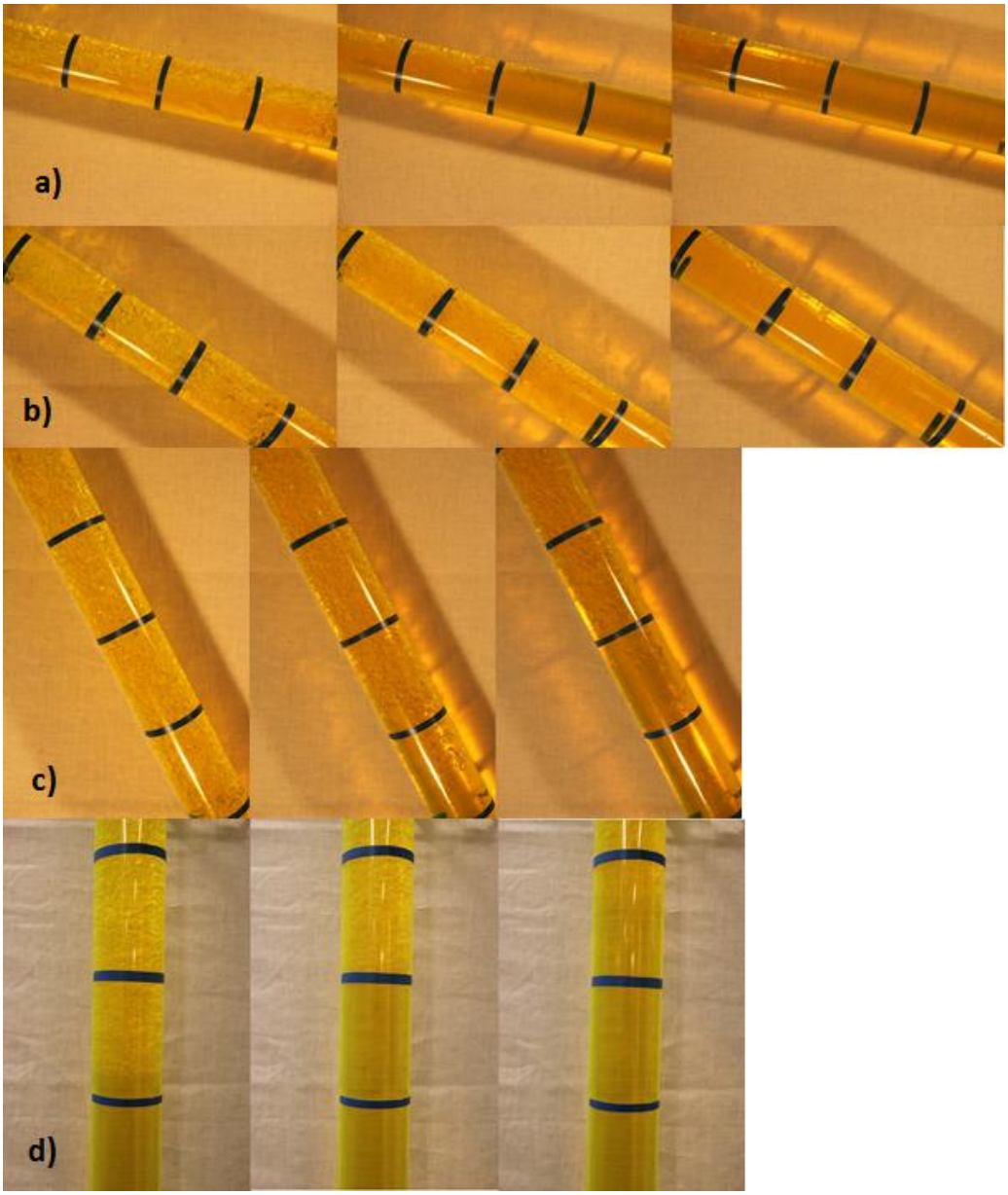

Figure 33 Photo series of the waterfront during *mixed* experiments using a 50mm ID cylinder at a) 10 degrees b) 30 degrees c) 60 degrees and d) 90 degrees inclination.

4.6.3 Vertically separated

4.6.3.1 Water front

Illustrated in Figure 34 is the progression of the water front at the angles 10, 30, 60 and 90 degrees. At 10 degrees it is evident that the oil and water phases flow separated and the water front is relatively stable, it has little tendency to break up. The water front is quite wavy and it is clear that the in situ holdup shows variation throughout the flow. At 30 degrees the oil and water phases are still relatively continuous, but the flow is more chaotic and some mixing occurs. At 60 degrees these tendencies are reinforced and the front is almost completely broken up. The section behind the front can be characterized as bubbly flow. But at this angle the major part of the oil and water phase flow is still channelized, the water flows at the bottom and the oil at the top. Finally at 90 degrees the front was divided into several big bubbles, the front was no long as clear, there is no obvious signs of channelization and section behind the front is totally dispersed.

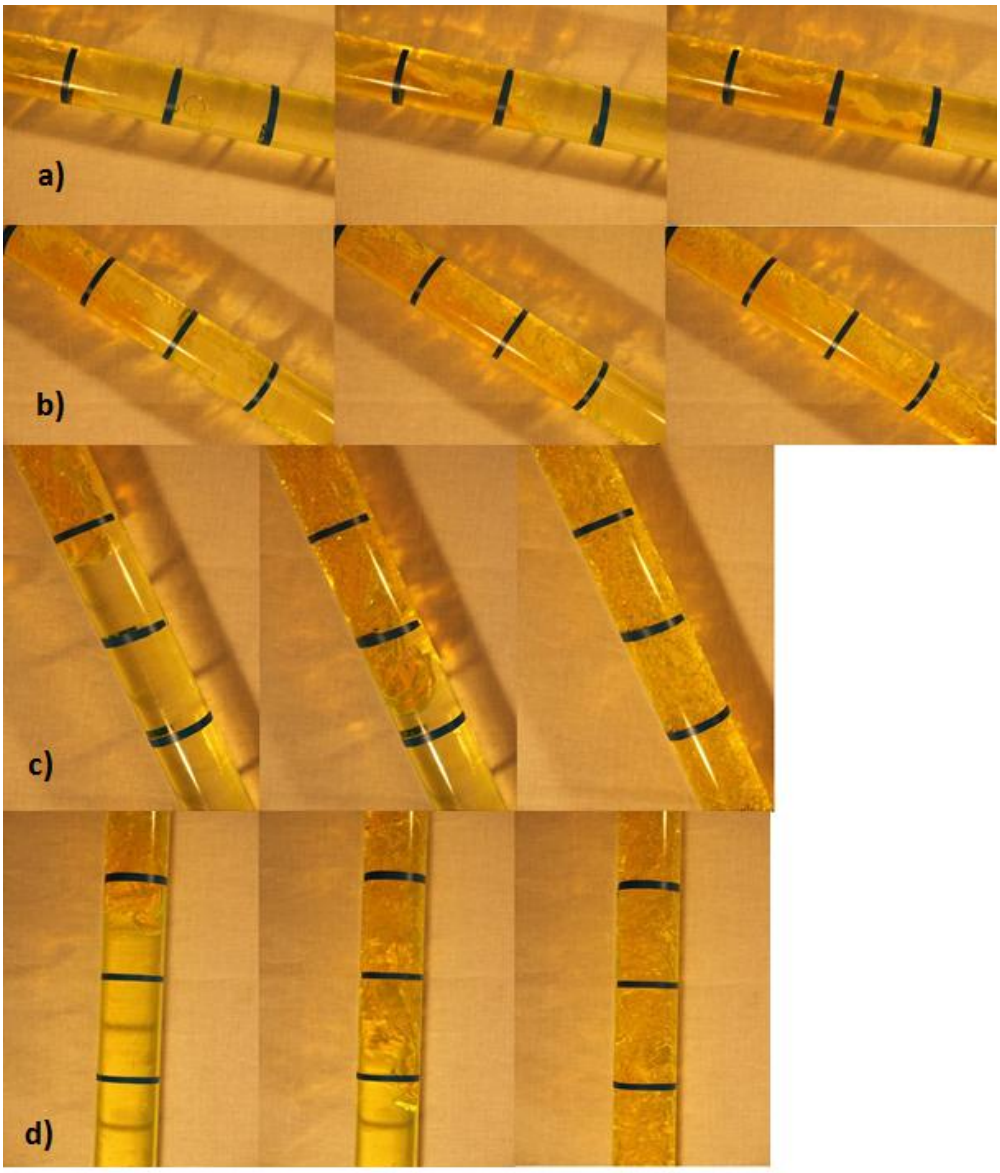

Figure 34 Illustrates the yellow water front as it flows down the cylinder for *vertically separated* experiments in a 50mm ID cylinder at a) 10 degrees b) 30 degrees c) 60 degrees and d) 90 degrees inclination.

4.6.3.2 Oil front

While the water front creeps down along the cylinder wall and is constantly changing appearance due to waves, the oil front remains a stable round bubble shape. This appearance is observed at all angles and the resemblance of a Taylor bubble is evident at 90° inclination as shown in Figure 35 d). The flow pattern behind the oil front is similar to that observed at the water front with separated flow at low angles and increasing mixing as the angle increases. However, it appears that there is more breakoff at the water front compared to the oil front.

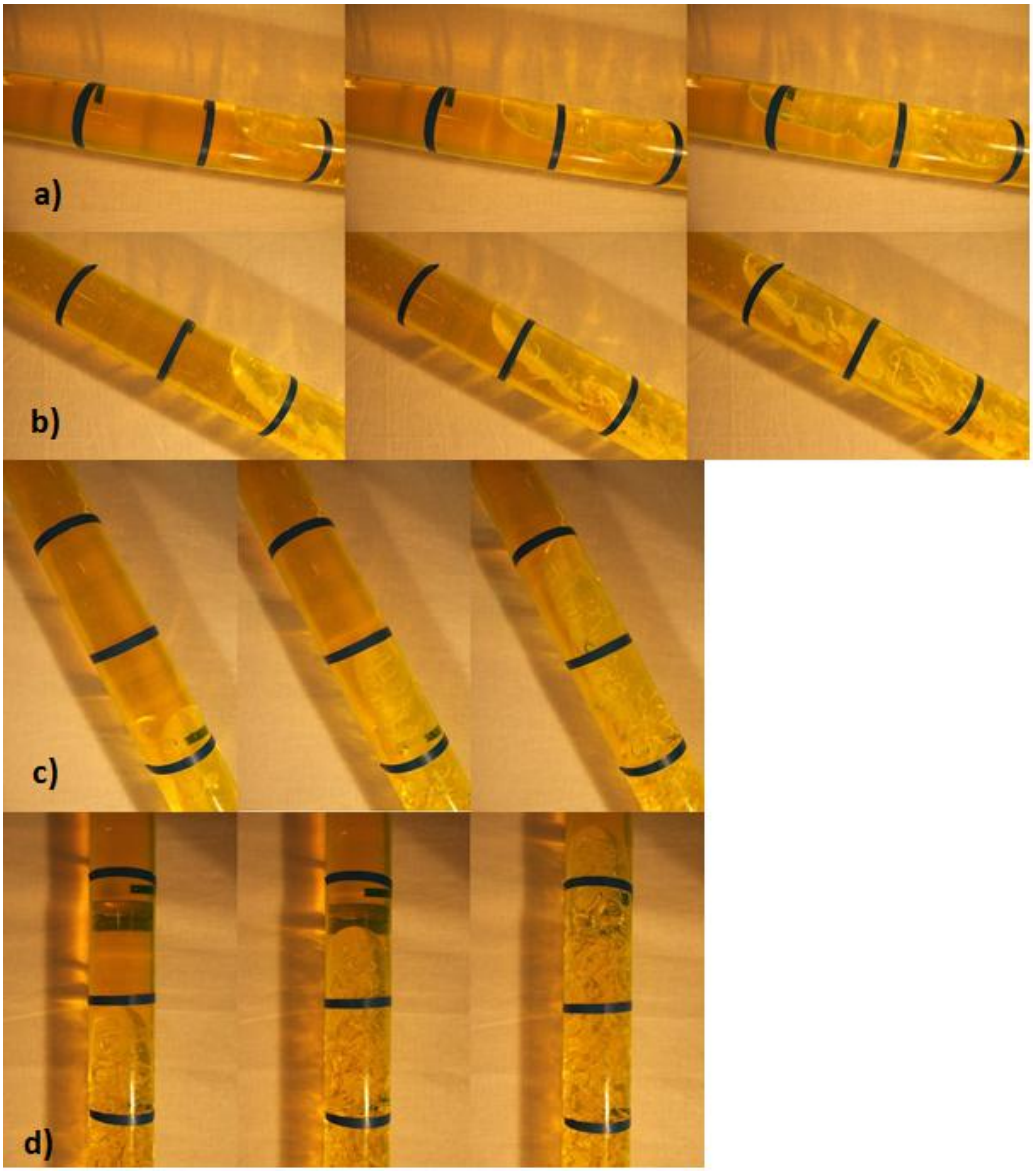

Figure 35 Illustrates the clear oil front as it flows upwards the cylinder for *vertically separated* experiments in a 50mm ID cylinder at a) 10 degrees b) 30 degrees c) 60 degrees and d) 90 degrees inclination.

.

4.6.4 Water Cut

4.6.4.1 Horizontal

The observed flow patterns in *horizontal* experiments at alternative water cuts were very similar to those observed with a 0.5 water cut with some differences. With 0.25 water cut at low inclination the phases remained separated and small waves were formed at the interface. No breakoff was observed. As the inclination increased, the waves became increasingly larger and some breakoff was observed at around 20 degrees inclination. At 50 degrees inclination the breakoff was so significant that the entire cross section of the cylinder was cluttered with bubbles. The bulk of flow was still channelized. At very high inclinations, channelization is still visible up until 90 degrees, but the entire flow was now chaotic and bubble dominated.

With 0.75 water cut, the observed flow patterns were similar to those at 0.25 water cut at low inclinations. At higher inclinations the oil phase appeared to have less tendency to enter the water phase, the oil phase did not extend as far into the water phase as the water phase extended into the oil phase in the previous experiment. At very high inclinations the oil phase appeared to be completely dispersed.

4.6.4.2 Mixed

For *mixed* experiments with alternative water cuts the observed flow patterns were quite different from those in the Base Case. With 0.25 water cut the phases were observed to separate quickly in the vertical direction. This happened so quickly that the phases appeared separated even before the cylinder was put into its final position. The water phase was still dominated by bubbles, but there was a large continuous oil phase surrounding it. At low inclinations, the phases remained separated and there was a slow moving "tail" of water bubbles. At higher inclinations the bubbles in the water phase tended to enter the oil phase and were often transported upwards. At very high inclinations, the flow appeared similar to that observed with a 0.5 water cut.

With 0.75 water cut the results of the mixing procedure were quite different from any previous experiments. The mixed zone only covered roughly ¾ of the cylinder as illustrated in Figure 36, whereas it covered the entire cylinder in the 0.25 water cut experiments. This mixed zone was surrounded by a continuous water phase and moved through it like a bubble. At high inclinations there was still a large continuous water phase surrounding the mixed zone, however the mixed zone now covered the entire cross section of the cylinder, channelization was less evident. At 90 degrees, the flow pattern appeared very similar to those observed in other experiments.

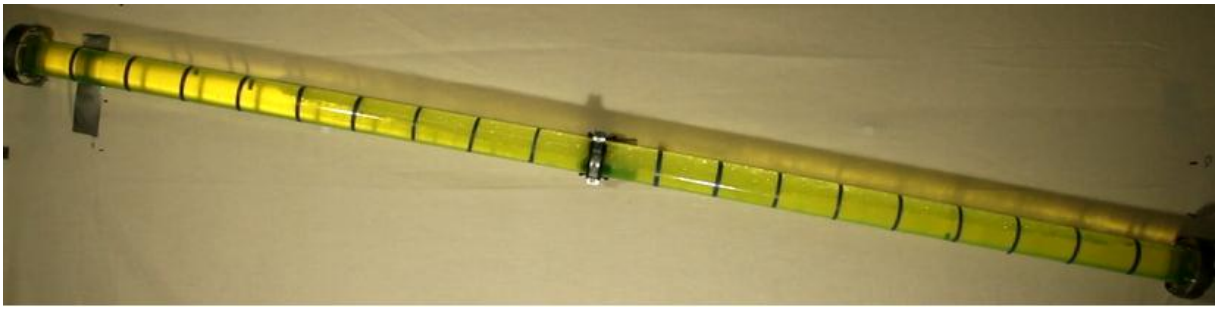

Figure 36 Photo of the mixed zone during Water Cut 0.75 *mixed* experiments at 10 degrees inclination.

4.6.5 Large Diameter

4.6.5.1 Horizontal

The same type of flow patterns were observed in the case of the large inner diameter cylinder compared to the small one. At low angles, i.e. 10 degrees, the flow remained completely separated, dominated by wave formation with little breakup. As the inclination increased, the waves started breaking up and at 40 degrees a mixed zone was effectively formed. This behavior continued with channelization being less and less present until 90 degrees. Although the general flow patterns were similar to those of the small cylinder, the large cylinder was found to be better suited for visual inspection with the simple setup that was used. However, due to somewhat higher velocities, the relative uncertainty remained similar to that of the smaller inner diameter.

4.6.5.2 Mixed

The Large Diameter *mixed* experiments were also quite similar to the Base Case. At low inclinations, the phases quickly separated in the vertical direction although perhaps more bubbles were observed in the case of the large inner diameter compared to the small one. A continuous water phase was seen at the bottom of the cylinder cross section and a continuous oil phase at the upper end with a mixed layer in between. As the inclination increased, the flow became more chaotic with increased presence of bubbles. At high inclinations, the signs of channelization became less evident and at a vertical position the phases were completely dispersed.

4.6.5.3 Vertically separated

Figure 37 shows the propagation of the water front for inclination angles, θ, of 10°, 30°, 60° and 90° for *vertically separated* experiments using Marcol 52 as the oil phase and in a 90mm ID cylinder. The same type of flow patterns are observed as for the small cylinder as shown in Figure 34. At 10° inclination, the phases remain separated, but some wave breakup is observed. At 30° the phases are still separated at the front, but they become more dispersed behind the front. At 60° the phases become dispersed immediately behind the front and at 90° the phases can be said to be completely dispersed.

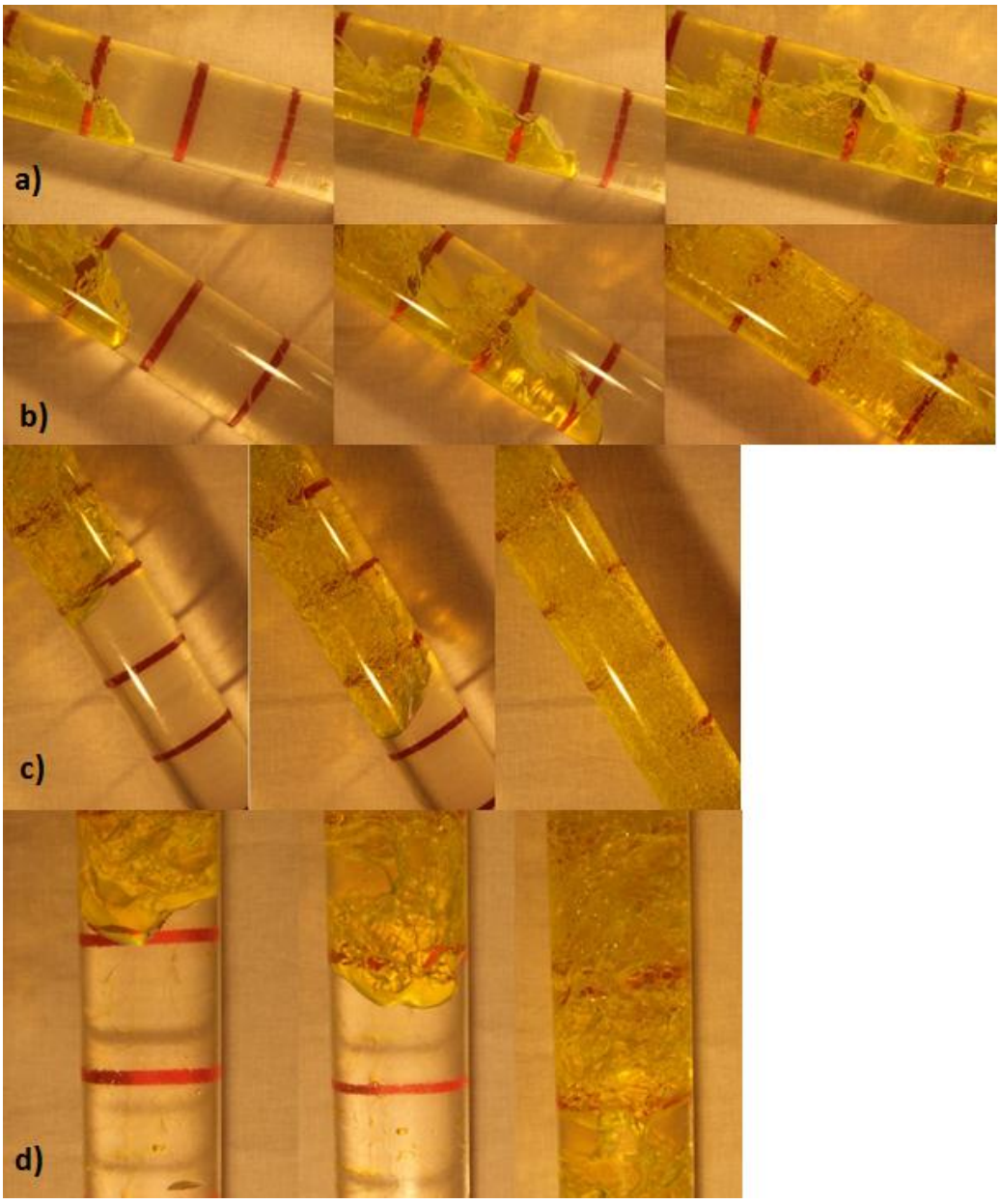

Figure 37 Photo series displaying the water front moving downwards in *vertically separated* experiments at a) 10 degrees b) 30 degrees c) 60 degrees and d) 90 degrees inclination in a 90mm ID cylinder

4.6.6 Oil Front

During all the experiments, there were some differences between the oil and water fronts as described in some of the previous sections. An overview picture as shown in Figure 38 may help illustrate some of these differences better. This example shows a *mixed* type experiment at 90° inclination where Marcol 52 is used as the oil phase in the 90mm ID cylinder and a 0.5 water cut. It is evident that the propagation of the two fronts is quite different as they approach separation. While the water front continues upwards with relatively constant speed, the oil front appears to stagnate due to the formation of foam. This illustrates one of the major problems with visual inspection, since one might say that in the last picture, the mixed zone appears to be quite large, roughly 50cm long. However, this mixed zone must contain a high amount of oil, since there is such a large continuous water zone.

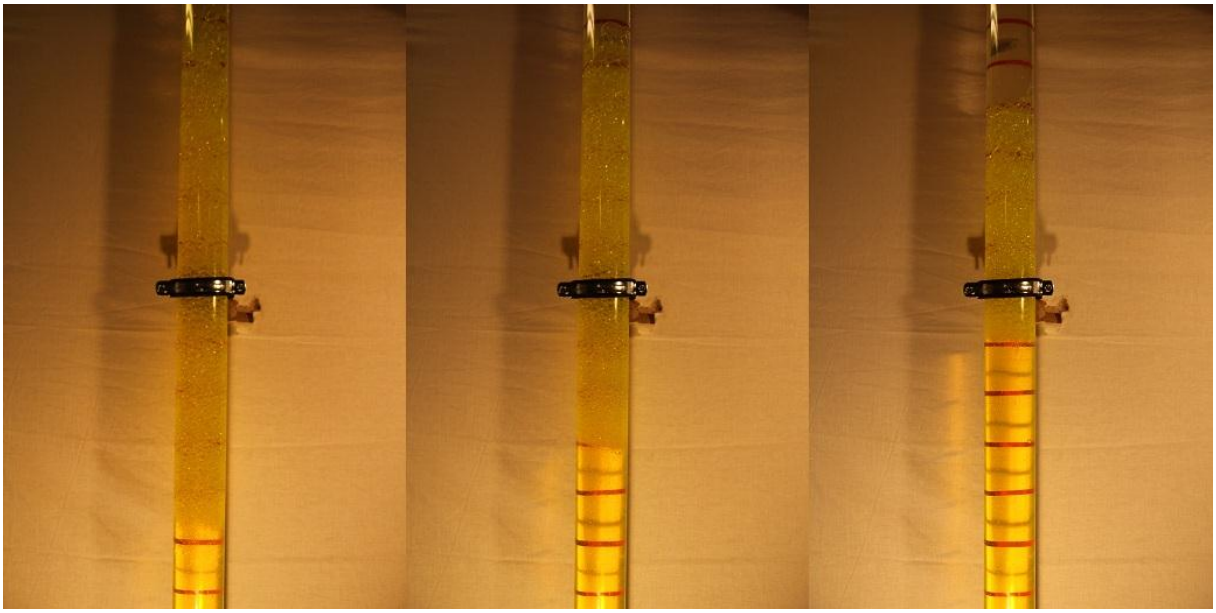

Figure 38 Overview of oil and water fronts during Large Diameter *mixed* experiments at 90° inclination.

5 Analysis and discussion

The slip velocity has been calculated for all experiments using Equation 2.7. The calculated slip velocities are compared for different sets of experiments to find the effects of individual experimental parameters.

5.1 Start conditions

The three different starting conditions were compared to each other to observe characteristics individual for each one, and to discuss the reason for these characteristics. To offer a broader perspective, the starting conditions are compared for all the experiments conducted.

5.1.1 Base Case

Figure 39 shows a comparison of estimated average slip velocities for *horizontal*, *mixed* and *vertically separated* starting conditions with Exxsol D80 as the oil phase in a 50mm ID cylinder. For all three types of experiments, the maximum slip velocity appears to be found at roughly the same inclination of about 10 to 25 degrees. They also share the same characteristic of dropping off towards a minimum point at 90 degrees inclination. The slip velocity found for *mixed* experiments remains roughly half of that found in *horizontal* experiments for all inclinations. The slip velocity found in *vertically separated* experiments appear to match well to those of *horizontal* experiments at inclinations from 5 to 30 degrees. At higher inclinations, the slip velocity drops off much faster in *vertically separated* experiments and the calculated slip velocity appears to be closer to that found in *mixed* experiments.

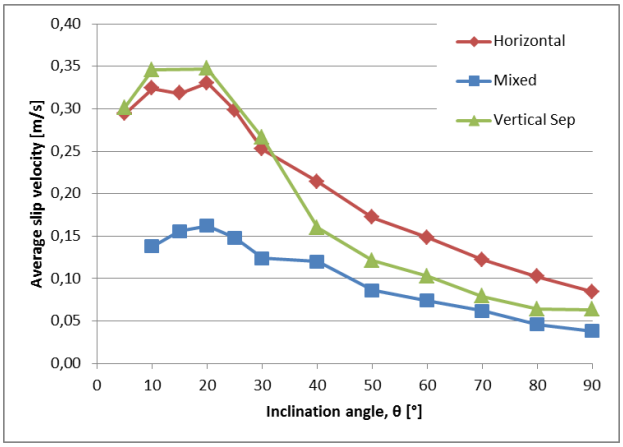

Figure 39 Comparison of average slip velocities for three different starting conditions for Base Case experiments.

5.1.2 Marcol 52 and Large Diameter

A similar comparison was performed on the experiments with Marcol 52 as the oil phase for both those in a 50mm and 90mm ID cylinder, illustrated in Figure 40 and Figure 41 respectively. Generally the same patterns are observed in both these figures as was seen in Figure 39, however there are some differences. The *horizontal* experiments have a lower slip velocity compared to *vertically separated* experiments at inclinations close to horizontal, 5 to 15 degrees, and the curves intercept at roughly 25 degrees for both cylinder sizes. The slip velocity from *vertically separated* experiments then approaches that of *mixed* experiments and at a vertical position they yield roughly the same slip velocity. This transition appears to be

quite abrupt in the case of Exxsol D80, but is very gradual in both cases with Marcol 52. There are no distinct differences between the 50mm ID cylinder and the 90mm ID cylinder experiments except that slip velocities at low angles are slightly higher for the large cylinder.

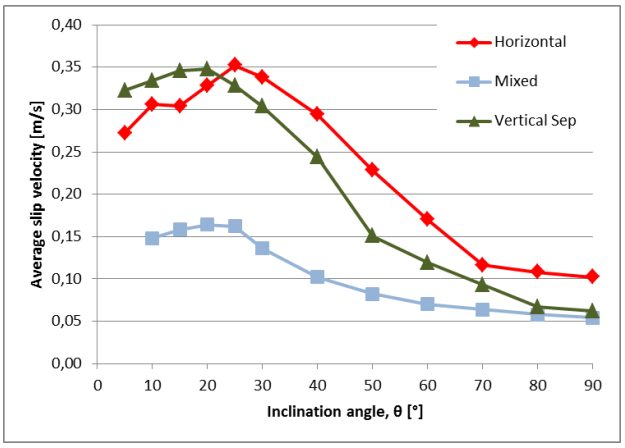

Figure 40 Comparison of average slip velocities for three different starting conditions for Marcol 52 experiments.

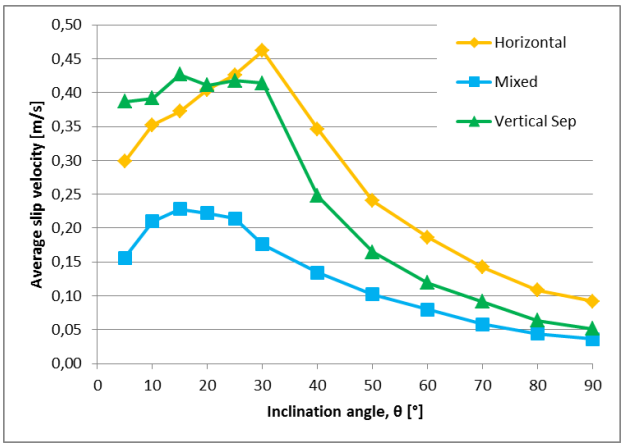

Figure 41 Comparison of average slip velocities for three different starting conditions for Large Diameter experiments.

5.1.3 Water Cut

The average slip velocities found in *mixed* and *horizontal* experiments for water cuts of 0.25 and 0.75 are displayed in Figure 42 and Figure 43. The average slip velocities calculated for the *horizontal* experiments with 0.25 water cut are significantly higher and display a different pattern when compared to the *mixed* experiments. For the *horizontal* experiments the slip velocity is initially low and increases toward a maximum point at around 25 degrees then subsequently declines toward a minimum point at 90 degrees inclination. The *mixed* experiments on the other hand yield an almost constant slip velocity in the interval between 10 and 30 degrees before steadily declining towards the minimum point at 90 degrees inclination.

The experiments using 0.75 as the water cut yields slip velocities that display somewhat similar curves both for *horizontal* and *mixed* experiments. Both curves initially increases before reaching a maximum at roughly 20-30 degrees inclination and then decreasing toward a minimum at 90 degrees inclination. Aside from the very low inclinations the values for *mixed* and *horizontal* slip velocities are relatively similar in magnitude, *mixed* yielding slightly lower slip velocities.

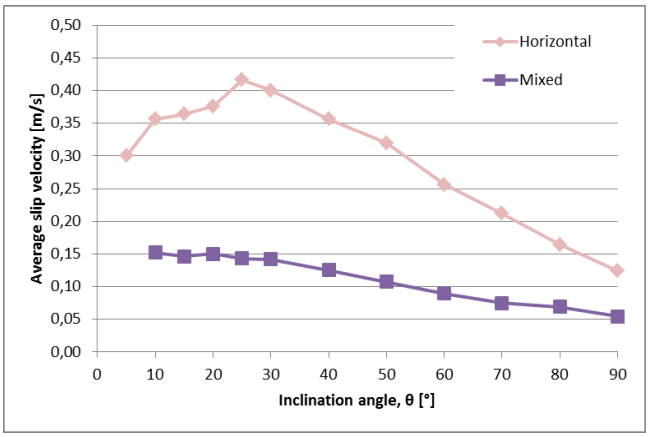

Figure 42 Comparison of average slip velocities for two different starting conditions for Water Cut 0.25 experiments.

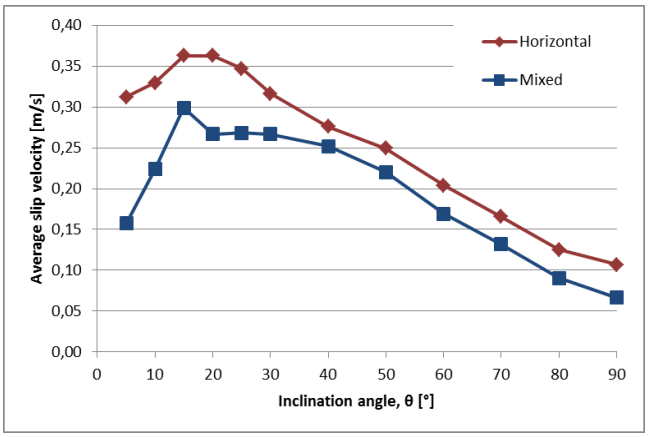

Figure 43 Comparison of average slip velocities for two different starting conditions for Water Cut 0.75 experiments.

5.1.4 Evaluation of starting conditions

It is important to note that the three different starting conditions yield inherently different types of experiments and some considerations must be taken when comparing them. The water front appears different in *horizontal* and *mixed* experiments due to the increased presence of bubbles in the latter type. The slip velocity found in *vertically separated* experiments is found based on a slightly different method compared to the other two, since the criteria for deciding the starting time is different as described in Section 3.3. At the start of phase two, the cylinder has been in the same inclination for a small period of time, removing the rotational effect in the beginning. However, the initial degree of mixing of the content varies much more with the inclination angle since the mixing is depending on this rather than on a constant mixing process as in *mixed* experiments.

With this being said, certain unique characteristics were identified for each starting condition. The *horizontal* experiments generally resulted in high slip velocities due to the low degree of mixing. The *mixed* experiments generally resulted in the lowest slip velocities at all angles even though a channeling effect was observed at almost all inclinations. The reason why *mixed* experiments give a lower slip velocity is because both oil and water phase are dominated by bubbles thus giving the phases larger surface area, increasing the interface friction.

Vertically separated experiments provide an insight in the mixing process and its dependency on inclination. The abrupt drop in slip velocity at 30 to 40 degrees inclination coincides with the observed mixing occurring at this point as described in Section 4.6.3. The drop in slip velocity appears more gradual relative to the other two curves for Marcol 52 and this could be an indication of the mixing process being different for the two oils. Finally, the slip velocities found for *vertically separated* experiments yield a close match to those of *mixed* experiments at a vertical position. This indicates that a similar degree of mixing is obtained in those two cases and that the five rotations used in the mixing process of *mixed* experiments did not yield much further mixing.

When looking at the experiments with 0.25 water cut, the same trends are observed as for the 0.5 water cut experiments, with *horizontal* yielding a high slip velocity and *mixed* yielding a comparatively low slip velocity. This is in contrast to the observations for experiments with a

0.75 water cut. As mentioned earlier, the slip velocity for *mixed* experiments in this case are almost as high as those for *horizontal*. The observed pattern is abnormal compared to what is observed in other experiments. The degree of mixing appears to be much lower even though the same mixing procedure was used.

5.2 Horizontal

To facilitate the effect of the experimental parameters, all the parameters are compared to the base case for *horizontal* experiments in this section. In Figure 44 the effects of changing oil and cylinder diameter are compared to the Base Case. The slip velocities for all three cases are roughly the same at 5 degree inclination and at 90 degree inclination. Marcol 52 and Exxsol D80 have similar slip velocities for the intervals 5-20º and 70-90º inclination. In the 20-70 degrees interval the slip velocities for Marcol 52 are higher. The 90mm ID cylinder has the maximum slip velocity at 30 degrees inclination and the slip velocities are higher than those for the 50mm ID cylinders for almost all inclinations.

Figure 45 illustrates a comparison of the Base Case, 0.25 and 0.75 water cut for *horizontal* experiments. Slip velocities at 5 degrees for all three water cuts are roughly the same. The Base Case has the lowest slip velocities for all inclinations above 10 degrees. Experiments with a 0.25 water cut generally yield the highest slip velocities, while 0.75 water cut is roughly in the middle of the other two.

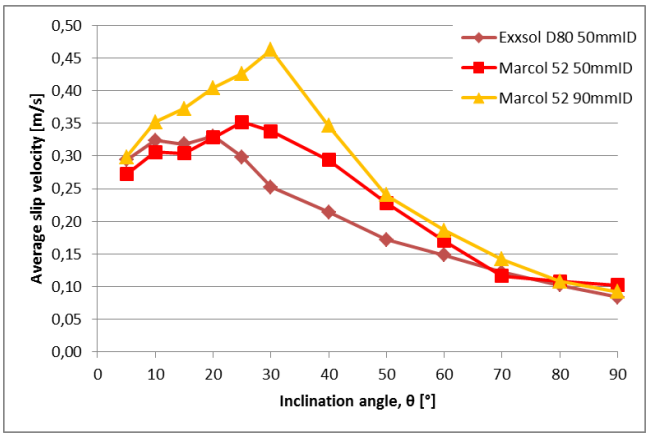

Figure 44 Average slip velocities for *horizontal* experiments for different oils and cylinder sizes.

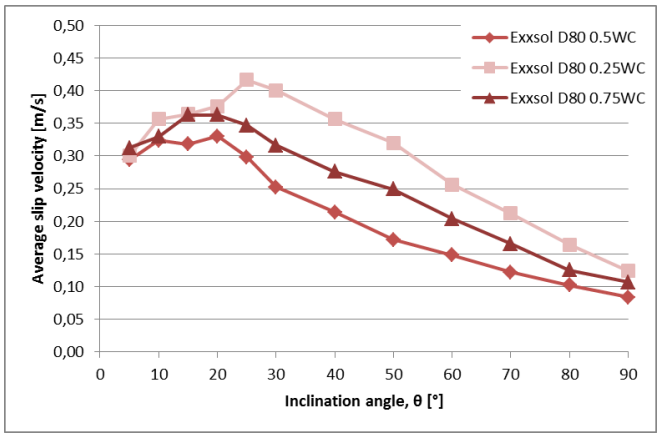

Figure 45 Average slip velocities for *horizontal* experiments for different water cuts.

The difference in slip velocities between Marcol 52 and Base Case experiments in the interval between 20 and 60 degrees inclination can be related to difference in the interaction between water and oil for the two oils. In both cases break offs began to appear around 20 degrees inclination and from then on only increased towards higher inclinations. However, a general observation was made that Exxsol D80 produces more bubbles, thus increasing the interfacial surface. The slip velocity found in the Large Diameter experiments is thought to be high at the low inclinations due to wall friction having less effect in a large diameter. At high inclinations, the interface friction between the phases will be the dominating force and it is thereby more similar to the 50mm ID.

In the Water Cut experiments it is interesting that both the alternative water cuts yield a generally higher slip velocity compared to the Base Case. In the Base Case experiments where

the oil to water content ratio is 1, there will be the highest possible interaction between the phases. Therefore this is expected to yield the lowest velocity.

5.3 Mixed

Resulting slip velocities for *mixed* experiments are compared in this section to identify which experimental parameters are impactful in this type of experiment. Figure 46 compares the results from the Base Case to those from Marcol 52 and the Large Diameter. Figure 47 compares the two alternative water cuts to the Base Case.

From Figure 46 it is evident that the slip velocities for Exxsol D80 and Marcol 52 are relatively similar in magnitude at all inclinations. The slip velocities in the large cylinder are considerably higher than the 50mm ID cylinder at low inclinations up until 40 degrees. At higher inclinations the slip velocity decreases and approaches the other two curves.

In the experiments with different water cuts the slip velocities for 0.5 and 0.25 water cuts are roughly the same for all inclinations with only minor deviations. The experiments with 0.75 water cut, however yield a slip velocity that is very high compared to the other two for all inclinations except at 80 and 90 degrees.

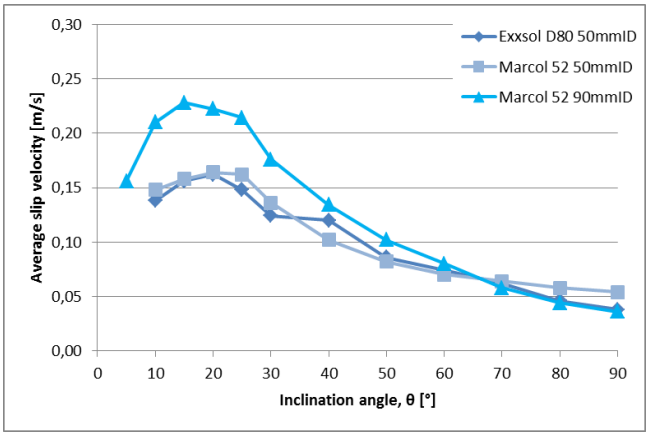

Figure 46 Average slip velocities for *mixed* experiments for different oils and cylinder sizes.

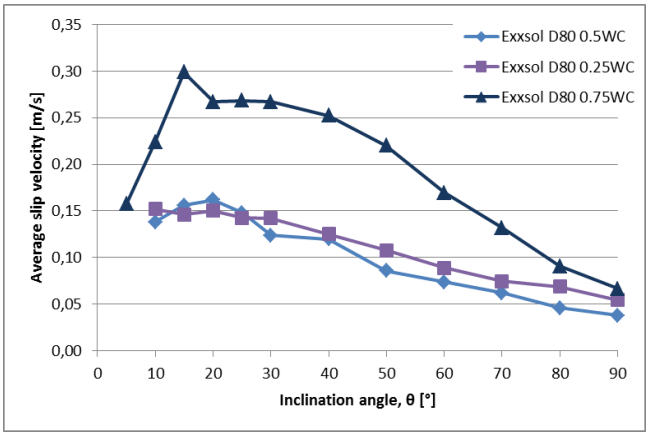

Figure 47 Average slip velocities for *mixed* experiments for different water cuts.

As indicated previously, there has been observed some differences in the mixing properties between Marcol 52 and Exxsol D80. In the case of *mixed* experiments no such difference is distinguishable, indicating that the two oils behave similarly when fully mixed. The Large Diameter experiments however, did yield a higher slip velocity for low inclinations compared to the two other cases. The reason for this is thought to be that at low inclinations the phases are less mixed, and wall friction is a more dominating force. In a large diameter cylinder, the circumference to area ratio is lower, causing the wall friction to be less impactful.

The slip velocities for 0.75 water cut experiments were exceptionally high. During these experiments a rather unique flow pattern was observed, this is described in Section 4.6.4.2. Since only a small mixed zone was formed there was less interface area, but this effect diminished at higher inclinations. It is also interesting that the slip velocity obtained at 0.25 water cut are similar to those at the Base Case.

5.4 Vertically separated

5.4.1 First phase

Average water and oil front velocities during the first phase for all *vertically separated* experiments are displayed in Figure 48. Even though the phases move in opposite directions, the front velocity is represented by a positive value in this figure. It is evident that there are some clear differences between the experimental classes. The Base Case, with Exxsol D80 as the oil phase, generally is characterized by a large difference between the water and oil front velocities. For Marcol 52 and Large Diameter experiments, the two fronts move at roughly the same velocity. The velocities are also much higher in the case of the 90mm ID cylinder compared to the 50mm ID for experiments with Marcol 52 as the oil phase.

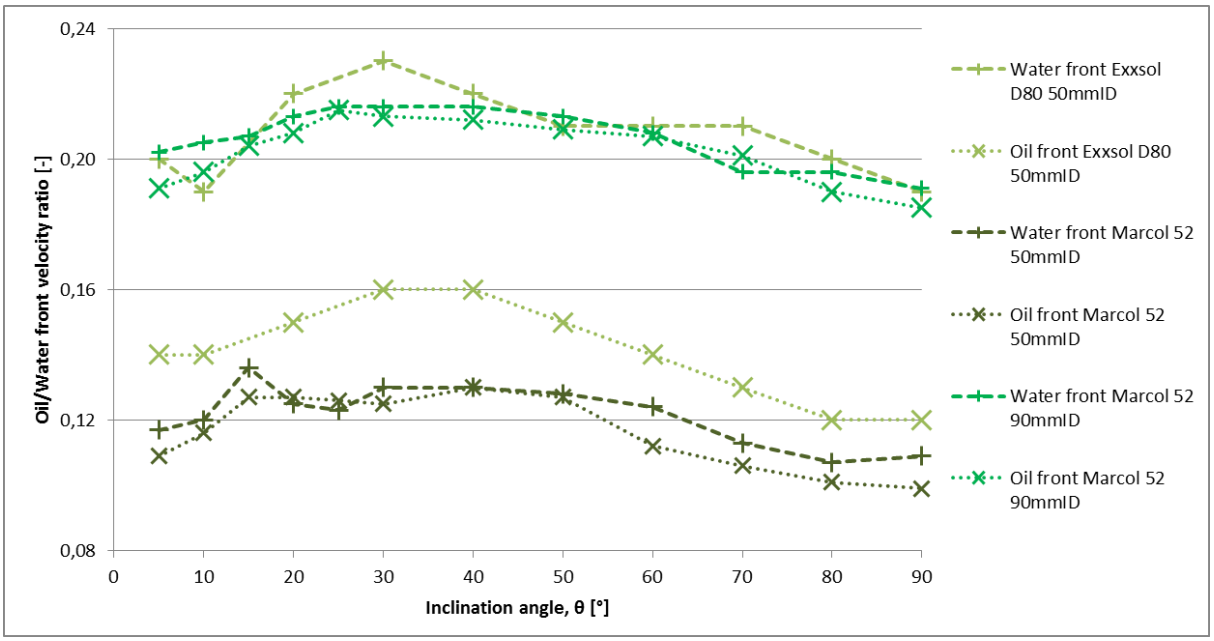

Figure 48 Average front velocities during the first phase of *vertically separated* experiments.

As shown in Figure 49, the oil to water front velocity ratio is consistently lower for Exxsol D80 experiments compared to Marcol 52. In the Marcol 52 experiments, both fronts would propagate at roughly the same speed, giving an O/W ratio of roughly 1. In the Exxsol D80 experiments, the water front moved consistently faster than the oil front and the O/W ratio was roughly 0.6-0.7.

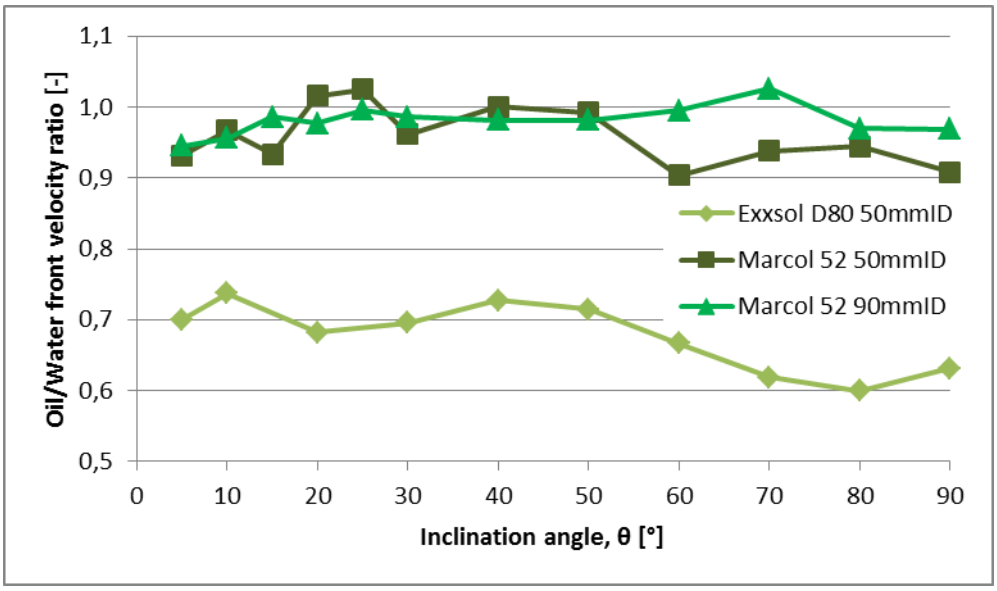

Figure 49 Oil to water velocity ratios for the first phase in *vertically separated* experiments.

In the first phase of these experiments, the phases remain completely separated except for the region between the two fronts where mixing occurs depending on the angle of inclination. From Figure 48 it is evident that the angle of inclination has some impact on the front velocities, but not nearly as much as observed in other types of experiments. The low velocities at low angles are caused by a small gravitational component. As the inclination increases the gravitational component becomes larger, but the shape of the front changes and the front area increases, as can be seen in Figure 37. This leads to increased interfacial friction and lower front velocities.

When comparing the Marcol 52 experiments to the Base Case it is evident that the water phase flows much faster in the Base Case. The oil phase also has a slightly higher velocity in the Base Case. The difference is very notable in the comparison of O/W ratios in Figure 49. The O/W ratio in the Base Case is around 0.6 to 0.7, somewhat varying for different inclinations, while the Marcol 52 and Large Cylinder experiments display a O/W ratio of roughly 1. This indicates that the cylinder diameter had little effect on the O/W ratio, but the oil phase shows a large difference. This can most likely be attributed to the large viscosity difference between the two oils.

The pipe diameter is seen to significantly affect the front velocities, however the oil to water front velocity ratio remains constant. This indicates that front velocities are highly impacted by wall friction.

5.4.2 Second phase

It is noteworthy that although such major differences are observed in the first phase on these experiments, this has little impact on the separation process in the second phase. The recorded separation times for each experiment are, as shown in Figure 50, quite similar regardless of both oil type and inner diameter size. The Base Case experiments appear to have somewhat longer separation time at angles between roughly 40 and 70 degrees. The calculated slip velocity which is based on the separation time is displayed in Figure 51. It is evident here that

the slip velocity is slightly higher for Large Diameter experiments at low angles up until roughly 40 degrees inclination.

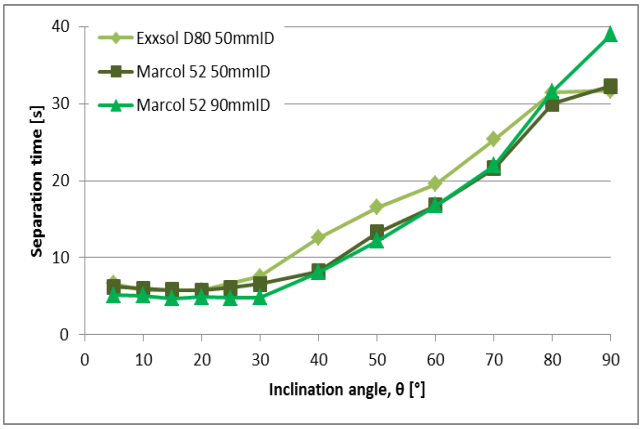

Figure 50 Separation times during the second phase of *vertically separated* experiments for three different cases.

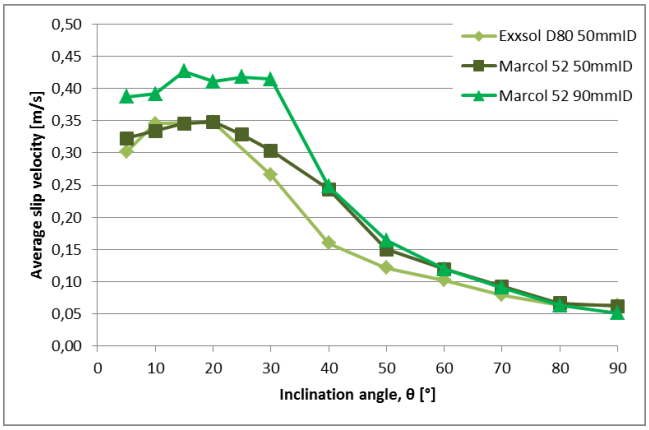

Figure 51 Average slip velocities for *vertically separated* experiments for different oils and cylinder sizes during the second phase.

The separation times during the second phase of *vertically separated* experiments are relatively similar, except in the inclinations between 40 and 70 degrees. This is the inclination region where the observed flow pattern was distorted for all experiments. A lot of bubbles were observed here compared to the lower inclination experiments, especially for experiments with Exxsol D80. This is believed to be the reason that the Exxsol D80 experiments separate slower. Since there is less wall friction in 90mm ID cylinder, the separation in these experiments is fast in the area where the wall friction is the dominating force. This results in a higher slip velocity for the low inclination area.

6 Discussion

6.1 Flow patterns

The observed flow patterns in these experiments are not surprisingly different from those observed for laminar counter-current flow by (Ullmann, Zamir, Ludmer, & Brauner, 2003). Completely separated flow with a stable interface was only observed for *horizontal* experiments at the very lowest angles of inclination, roughly 0-15 degrees. In their experiments, separated flow with a stable interface was obtained until roughly 60-70 degrees from the horizontal. Those experiments were performed with a density ratio near unity, roughly 0.95 whereas in our experiments, the difference in density between oil and water phase was larger with a density ratio of roughly 0.80. Since gravity is the driving force in this type of flow, the experiments with the highest density difference may lead to higher velocities and thereby increased turbulence and phase dispersion. The oil phase used in their experiments had a lower viscosity than the water-rich phase, in large contrast to our experiments where the oil phase had a higher viscosity than the water phase. There is also a large difference in the interfacial tension where our experiments had an interfacial tension almost ten times higher. Finally, their experiments had water and oil phase inlets at the top and the bottom of the cylinder giving a steady-state flow, opposed to the enclosed system with transient flow in our experiments. It is rather difficult to say which of these factors contribute towards yielding different flow patterns.

It is evident that the results from counter-current gas-liquid flows vary significantly from what is observed in our experiments with liquid-liquid flow. In gas-liquid flow, different researchers have identified the following flow patterns. For vertical flow the main flow patterns were annular flow, bubbly flow and slug flow (Taitel & Barnea, 1983). At off-vertical inclinations, slug, churn-stratified and semi-stratified flow patterns were observed (Ghiaasiaan, Wu, Sadowski, & Abdel-khalik, 1997). And at near horizontal inclinations the main flow pattern was stratified flow (Prayitno, Santoso, Deendarlianto, Höhne, & Lucas, 2012). In our experiments the observed flow patterns were stratified for low inclinations, three-layer and dispersed flow with channelization for intermittent inclinations and fully dispersed flow with no signs of channelization for vertical inclinations. No tendencies towards slug flow or annular flow were observed in any of our experiments. However we cannot exclude that such flow patterns may arise with a different setup of for example larger scale. We also were unable to find any gas-liquid transient flow experiments to compare with.

6.2 Front velocity

The front velocity measurements are influenced by a series of factors that cause uncertainties in the readings. Some of these factors, which were summarized in section 3.4, can be classified as random errors and a rough estimate of these are given by the data spread illustrated in the figures in the results section. The remainder of errors cannot be quantified in the same way, but are important to keep in mind when using the results of this research. The measured front velocities still give a rough model and the qualitative patterns observed will most likely remain the same with more precise measurements.

It is evident that in our experiments the local front velocity can vary quite significantly throughout the experiment. The reliability of local front velocity measurements was often very low, especially at low angles where the velocity was high and the front was less defined. In order to get more reliable values for the local front velocity profile at these angles, a more advanced experimental setup is required. However, we could establish that the measured initial local front velocity was very high due to either separation happening before the start of experiments or due to non-uniform mixing or both. We also noted that the local front velocity dropped towards zero during the last 20cm of the pipe due to foam and bubbles. These last 20cm therefore may have a large impact on the average front velocity, especially since it becomes difficult to define the point of when to say that the phases are fully separated.

6.3 Experimental Setup

Most petroleum related multiphase flow occurs in steel pipes. According to (Angeli & Hewitt, Flow structure in horizontal oil-water flow, 2000) the flow pattern is dependent on surface material and increased tendencies towards dispersions have been observed in stainless steel pipes. In our research, a Plexiglas cylinder was used, possibly yielding somewhat different flow patterns than what would occur in a real situation.

The pipe length may also impact the flow patterns. As seen in section 4.5, the local front velocity was continuously changing throughout experiments. This may indicate that starting and ending conditions have a relatively large impact on the flow when using such a short cylinder. If the flow occurred over a longer distance, a different velocity that is less impacted by these end conditions may be observed.

7 Conclusion

Transient inclined counter-current oil-water flow experiments have been conducted at the multiphase flow laboratory at The Norwegian University of Science and Technology, NTNU. Visual observations of flow patterns have been obtained for 755 experiments with different flow parameters, to establish slip relations that are to be implemented in a dynamic multiphase flow simulator.

- Four different flow patterns have been identified for this type of flow; Stratified flow, three layer flow, dispersed flow with channelization and fully dispersed flow.

- At inclinations up to 40 degrees the slip velocity is generally higher for a larger cylinder inner diameter. The effect is not evident for inclinations above this point, where the interfacial friction becomes dominant.

- Even at slightly off-vertical inclinations channelization was observed, however the impact on the slip velocity was small.

- The lowest separation time and thereby the highest slip velocities were obtained for inclinations between 15 and 30 degrees for all experiments.

- The lowest slip velocities were found at 90 degree inclinations for all experiments.

- The initial degree of mixing has a significant impact on the separation time.

- The water front proved more suitable to track visually due to it generally being more defined compared to the oil front.

- Experiments using alternative water cuts were found to be difficult to relate to each other due to large deviations in mixing resulting from the same mixing procedure.

8 Further Work

Since there is almost no available research on transient counter-current liquid-liquid flow, a lot of work remains in this field. This research has given a rough overview of the observed flow patterns and effects of many different parameters. If it proves to be necessary to have more precise measurements, we do have some recommendations for improvements based on what we have experienced over the course of this research.

Naturally there is some level of subjectivity involved in experiments based on visual inspection. It is difficult to classify and quantify observations in a manner that allows for good correlation with the works of other scientists. It could be desirable to implement a set of sensors to get objective observations of the flow. This would allow for an objective definition of the oil and water fronts as well as give valuable information about the mixed zone, such as the degree of mixing and the distribution of the phases. The mixed zone was generally so obscure that it was very difficult to make any meaningful visual observations about it.

The experiments could be performed on a pipe section of a larger system to better simulate natural flow patterns. The pipe section should have shutoff valves mounted on each end so the flow could be shut in. This would generate a more realistic mixing of the flow and eliminate discrepancies associated with the mixing procedure. Mounting the pipe section with flexible bends could allow for multiple inclinations to be tested and the water cut could be altered by changing the flow rates.

It is also suggested that these types of experiments are performed in a longer pipe segment. The local front velocity was found to vary significantly throughout experiments and was suspected to be heavily influenced by starting and ending conditions. Preforming the experiments on a longer pipe section would diminish the relative effect of the start and end condition.

As crude oil has a broad spectrum of physical properties, executing the experiments with a wider range of fluids could yield different slip velocities. The oils used in our experiments were relatively similar and yielded relatively similar flow patterns and slip velocities.

9 References

Angeli, P. (1994). Pressure Drop and Flow Patterns in Horizontal Liquid-Liquid Flow in Pipes. *Department of Chemical Engineering & Chemical Technology Imperial College of Science, Technology and Medicine Prince Consort Road London*.

Angeli, P., & Hewitt, G. F. (2000). Flow structure in horizontal oil-water flow. *International Journal of Multiphase Flow 26*, pp. 1117-1140.

Arirachakaran, S., Oglesby, K. D., Malinowsky, M. S., Shoham, O., & Brill, U. (1989, March 13-14). An Analysis of Oil/Water Flow Phenomena in Horizontal Pipes. *SPE Production Operations Symposium, Oklahoma City, Oklahoma, USA*.

Brauner, N., & Maron, D. M. (1992). Flow Pattern Transitions in Two-Phase Liquid-Liquid Flow in Horizontal Tubes. *International Journal of Multiphase Flow Vol 18, No 1*, pp. 123-140.

Danielson, T. J. (2007). Sand Transport Modeling in Multiphase Pipelines. *Offshore Technology Conference.* Houston, Texas USA.

Durlofsky, L. J., & Aziz, K. (2004). *Advanced Techniques for Reservoir Simulation and Modeling of Nonconventional Wells.* Stanford, CA: Department of Petroleum Engineering, Stanford University.

Fairuzov, Y. V. (2003). Transient gravity driven countercurrent two-phase liquid-liquid flow in horizontal and inclined pipes. *International Journal of Multiphase Flow, Vol. 29*, pp. 1759-1769.

Flores, J. G., Chen, T., Sarica, C., & P, B. J. (1999, May). Characterization of Oil-Water Flow Patterns in Vertical and Deviated Wells. *SPE Production & Facilities Vol 14, No 2*, pp. 94-101.

Ghiaasiaan, S. M., Wu, X., Sadowski, D. L., & Abdel-khalik, S. I. (1997, November). Hydrodynamic characteristics of counter-current two-phase flow in vertical and inclined channels: effects of liquid properties. *International Journal of Multiphase Flow 23*, pp. 1063-1083.

Hasan, A. R., Kabir, C. S., & Srinivasan, S. (1994, August). Countercurrent Bubble and Slug Flows in a Vertical System. *Chemical Engineering Science Vol. 49 Issue 16*, pp. 2567-2574.

Jepson, W. P., & Tayler, R. E. (1993). Slug Flow and its Transitions in Large Diameter Horizontal Pipes. *International Journal of Multiphase Flow Vol. 19*, pp. 411-420.

Nigan, K. H., Ioannou, K., Rhyne, L. D., Wang, W., & Angeli, P. (2009, March). A methodology for predicting phase inversion during liquid-liquid dispersed pipeline flow. *Chemical Engineering Research and Design, Volume 87, Issue 3*, pp. 318-324.

Plasencia, J., & Nydal, O. J. (2010). Influence of the pipe diameter in dispersed oil-water flows. *7th International Conference on Multiphase Flow.* Tampa, FL USA.

Prayitno, S., Santoso, R., Deendarlianto, Höhne, T., & Lucas, D. (2012). Counter Current Flow Limitations of Gas-Liquid Two-Phase Flow in Nearly Horizontal Pipe. *Science and Technology of Nuclear Installations*.

Shi, H., Holmes, J. A., Aziz, K., Diaz, L. R., Alkaya, B., & Oddie, G. (2005, March). Drift-flux Modeling of Two-Phase Flow in Wellbores. *SPE Journal Vol 10, No.1*, pp. 24-33.

Taitel, Y., & Barnea, D. (1983, Dec). Counter current gas-liquid vertical flow, model for flow pattern and pressure drop. *International Journal of Multiphase Flow 9*, pp. 637-647.

Ullmann, A., Zamir, M., Ludmer, Z., & Brauner, N. (2003). Stratified laminar countercurrent flow of two liquid phases in inclined tubes. *International Journal of Multiphase Flow 29*, pp. 1583-1604.

Vedapuri, D., Bessette, D., & Jepson, W. P. (1997). A Segregated Flow Model to Predict Water Layer Thickness in Oil-Water Flows in Horizontal and Slightly Inclined Pipes. *BHR Group Multiphase.*

Wongwises, S. (1998). Interfactial friction factors in countercurrent stratified two-phase flow in a nearly-horizontal circular pipe. *International Communications in Heat and Mass Transfer*, pp. 369-377.

Xu, J.-Y., Wu, Y.-x., Feng, F.-f., Chang, Y., & Li, D.-h. (2008). Experimental investigation on the slip between oil and water in horizontal pipes. *Experimental Thermal and Fluid Science 33*, pp. 178-183.

Yusuf, N., Al-Wahaibi, Y., Al-Wahaibi, T., Al-Ajmi, A., Olawale, A., & Mohammed, I. (2011, Dec). Effect of oil viscosity on the flow structure and pressure gradient in horizontal oil-water flow. *Chemical Eng. Res.*, p. doi: 10.1016/j.cherd.2011.11.013.

Appendix A

A summary of measured average front velocities from all the experiments.

50mm ID

Exxsol D80

Inclination	0.5 Water Cut				0.25 Water Cut				0.75 Water Cut			
	Mixed		Horizontal		Mixed		Horizontal		Mixed		Horizontal	
	Ub avg	*Data Spread(±)*	**Ub avg**	*Data Spread(±)*	**Ub avg**	*Data Spread(±)*	**Ub avg**	*Data Spread(±)*	**Ub avg**	*Data Spread(±)*	**Ub avg**	*Data Spread(±)*
5			**0,147**	*0,028*			**0,075**	*0,003*	**0,118**	*0,013*	**0,234**	*0,019*
10	**0,069**	*0,006*	**0,162**	*0,016*	**0,038**	*0,006*	**0,089**	*0,008*	**0,168**	*0,027*	**0,247**	*0,038*
15	**0,078**	*0,008*	**0,159**	*0,024*	**0,037**	*0,004*	**0,091**	*0,008*	**0,224**	*0,014*	**0,272**	*0,013*
20	**0,081**	*0,012*	**0,165**	*0,029*	**0,038**	*0,003*	**0,094**	*0,011*	**0,200**	*0,026*	**0,272**	*0,040*
25	**0,074**	*0,011*	**0,149**	*0,016*	**0,036**	*0,006*	**0,104**	*0,010*	**0,201**	*0,023*	**0,260**	*0,039*
30	**0,062**	*0,008*	**0,126**	*0,011*	**0,036**	*0,004*	**0,100**	*0,021*	**0,200**	*0,028*	**0,237**	*0,020*
40	**0,060**	*0,009*	**0,107**	*0,017*	**0,031**	*0,003*	**0,089**	*0,025*	**0,189**	*0,006*	**0,207**	*0,020*
50	**0,043**	*0,002*	**0,086**	*0,006*	**0,027**	*0,004*	**0,080**	*0,015*	**0,165**	*0,015*	**0,187**	*0,016*
60	**0,037**	*0,002*	**0,074**	*0,007*	**0,022**	*0,003*	**0,064**	*0,008*	**0,127**	*0,009*	**0,153**	*0,014*
70	**0,031**	*0,002*	**0,061**	*0,008*	**0,019**	*0,001*	**0,053**	*0,007*	**0,099**	*0,012*	**0,124**	*0,006*
80	**0,023**	*0,002*	**0,051**	*0,003*	**0,017**	*0,002*	**0,041**	*0,002*	**0,068**	*0,005*	**0,094**	*0,004*
90	**0,019**	*0,002*	**0,042**	*0,009*	**0,014**	*0,002*	**0,031**	*0,006*	**0,050**	*0,004*	**0,080**	*0,009*

50mm ID

Marcol

0.5 Water Cut

Inclination	Mixed		Horizontal	
	Ub avg	*Data Spread(±)*	**Ub avg**	*Data Spread(±)*
5			**0,136**	*0,004*
10	**0,074**	*0,015*	**0,153**	*0,023*
15	**0,079**	*0,034*	**0,152**	*0,022*
20	**0,082**	*0,009*	**0,164**	*0,022*
25	**0,081**	*0,003*	**0,176**	*0,036*
30	**0,068**	*0,011*	**0,169**	*0,007*
40	**0,051**	*0,005*	**0,147**	*0,028*
50	**0,041**	*0,006*	**0,114**	*0,012*
60	**0,035**	*0,002*	**0,085**	*0,011*
70	**0,032**	*0,002*	**0,058**	*0,007*
80	**0,029**	*0,003*	**0,054**	*0,007*
90	**0,027**	*0,006*	**0,051**	*0,007*

90mm ID

Marcol

0.5 Water Cut

Mixed		Horizontal	
Ub avg	*Data Spread(±)*	**Ub avg**	*Data Spread(±)*
0,078	0,028	**0,149**	*0,004*
0,105	0,009	**0,176**	*0,013*
0,114	0,021	**0,186**	*0,034*
0,111	0,012	**0,202**	*0,016*
0,107	0,021	**0,213**	*0,041*
0,088	0,007	**0,231**	*0,033*
0,067	0,016	**0,173**	*0,024*
0,051	0,012	**0,120**	*0,005*
0,04	0,007	**0,093**	*0,007*
0,029	0,003	**0,071**	*0,010*
0,022	0,004	**0,054**	*0,004*
0,018	0,004	**0,046**	*0,003*

Vertically Separated	*50mmID*										
	Exxsol D80								**Marcol 52**		
	First phase			Second phase					First phase		
Angle (deg)	Ubo [m/s]	Ubw [m/s]	**O/W ratio**	**Sep time**	*Data Spread (±)*	**Ub avg**	*Data Spread (±)*		Ubo [m/s]	Ubw [m/s]	**O/W ratio**
5	0,14	0,20	**0,70**	**6,64**	*0,45*	**0,151**	*0,010*		0,11	0,12	**0,93**
10	0,14	0,19	**0,74**	**5,79**	*0,7*	**0,173**	*0,021*		0,12	0,12	**0,97**
15									0,13	0,14	**0,93**
20	0,15	0,22	**0,68**	**5,76**	*0,81*	**0,174**	*0,025*		0,13	0,13	**1,02**
25									0,13	0,12	**1,02**
30	0,16	0,23	**0,70**	**7,53**	*1,21*	**0,133**	*0,022*		0,13	0,13	**0,96**
40	0,16	0,22	**0,73**	**12,54**	*1,62*	**0,080**	*0,010*		0,13	0,13	**1,00**
50	0,15	0,21	**0,71**	**16,51**	*1,79*	**0,061**	*0,007*		0,13	0,13	**0,99**
60	0,14	0,21	**0,67**	**19,52**	*2,25*	**0,051**	*0,006*		0,11	0,12	**0,90**
70	0,13	0,21	**0,62**	**25,31**	*1,18*	**0,040**	*0,002*		0,11	0,11	**0,94**
80	0,12	0,20	**0,60**	**31,43**	*0,64*	**0,032**	*0,001*		0,10	0,11	**0,94**
90	0,12	0,19	**0,63**	**31,67**	*2,06*	**0,032**	*0,002*		0,10	0,11	**0,91**

Vertically Separated	*50mmID*				*90mmID*						
	Marcol 52				**Marcol 52**						
	Second phase				First phase			Second phase			
Angle (deg)	**Sep time**	*Data Spread (±)*	**Ub avg**	*Data Spread (±)*	Ubo [m/s]	Ubw [m/s]	**O/W ratio**	**Sep time**	*Data Spread (±)*	**Ub avg**	*Data Spread (±)*
5	**6,2**	*0,45*	**0,161**	*0,012*	0,19	0,20	**0,95**	**5,17**	*0,56*	**0,193**	*0,021*
10	**5,99**	*0,65*	**0,167**	*0,018*	0,20	0,21	**0,96**	**5,11**	*0,9*	**0,196**	*0,036*
15	**5,79**	*1,09*	**0,173**	*0,034*	0,20	0,21	**0,99**	**4,69**	*1,72*	**0,213**	*0,090*
20	**5,75**	*0,78*	**0,174**	*0,024*	0,21	0,21	**0,98**	**4,87**	*1,2*	**0,205**	*0,054*
25	**6,09**	*1,04*	**0,164**	*0,029*	0,22	0,22	**1,00**	**4,79**	*0,92*	**0,209**	*0,042*
30	**6,59**	*1,09*	**0,152**	*0,026*	0,21	0,22	**0,99**	**4,83**	*0,55*	**0,207**	*0,024*
40	**8,22**	*1,15*	**0,122**	*0,017*	0,21	0,22	**0,98**	**8,08**	*0,36*	**0,124**	*0,006*
50	**13,3**	*2,65*	**0,075**	*0,016*	0,21	0,21	**0,98**	**12,18**	*1,99*	**0,082**	*0,014*
60	**16,78**	*3,13*	**0,060**	*0,012*	0,21	0,21	**1,00**	**16,77**	*2,13*	**0,060**	*0,008*
70	**21,58**	*1,54*	**0,046**	*0,003*	0,20	0,20	**1,03**	**21,96**	*2,31*	**0,046**	*0,005*
80	**29,95**	*2,14*	**0,033**	*0,002*	0,19	0,20	**0,97**	**31,52**	*5,03*	**0,032**	*0,005*
90	**32,24**	*4,74*	**0,031**	*0,005*	0,19	0,19	**0,97**	**38,98**	*6,77*	**0,026**	*0,005*